

Exploring the Use of Instrumented Insoles to Estimate Trunk Local Dynamic Stability During Treadmill Walking

Alexandre Mir-Orefice

Thesis submitted to the University of Ottawa
in partial Fulfillment of the requirements for the
Master of Science in Human Kinetics

School of Human Kinetics
Faculty of Health Sciences
University of Ottawa

© Alexandre Mir-Orefice, Ottawa, Canada, 2023

Table of Contents

Table of Contents	ii
Acknowledgements.....	iv
List of Tables	vi
List of Figures.....	vii
List of Equations.....	viii
Definition of Terms.....	ix
Abstract.....	x
Chapter 1: Introduction.....	1
Chapter 2: Literature Review.....	5
2.1 Falls.....	5
2.2 Gait.....	5
2.2.1 Gait Stability	8
2.2.2 Measures of Gait Stability	9
2.2.2.1 Variability Metrics	11
2.2.2.2 The Maximum Finite-Time Lyapunov Exponent.....	13
2.2.3 Trunk Stability	17
2.3 Motion Capture	19
2.3.1 Inertial Measurement Units.....	20
2.3.2 Instrumented Insoles	22
2.4 Statistical Analyses	24
2.4.1 Intraclass Correlation Coefficients	24
2.4.2 Multiple Linear Regression.....	26
2.5 Summary.....	29
Chapter 3: Purpose.....	30
Chapter 4: Hypothesis.....	30
Chapter 5: Methods.....	31
5.1 Participants.....	31
5.2 Participant Preparation.....	32
5.3 Data Protocol	33
5.4 Data Processing.....	34
5.4.1 Gait Detection	35
5.4.2 Calculating Variability.....	36

5.4.2.1 Spatiotemporal Variability.....	37
5.4.2.2 Kinematic Variability.....	39
5.4.3 Calculating Local Dynamic Stability.....	41
5.5 Statistical Analysis.....	42
Chapter 6: Results.....	45
6.1 Metric Calculation	45
6.2 Local Dynamic Stability Correlations	46
6.3 Multiple Linear Regression.....	47
Chapter 7: Discussion	52
Chapter 8: Limitations	60
Chapter 9: Future work	62
Chapter 10: Conclusion.....	63
Chapter 11: References	64
Appendix A: Research Consent Form	80
Appendix B: Anthropometric measurements.....	84
Appendix C: Instrumented-insole design.....	85
Appendix D: Median Absolute Deviation of Yaw Variability Calculation.....	86
Appendix E: List of Metrics	87

Acknowledgements

The work presented in this thesis was the result of hard work and support from multiple parties and wonderful people. I am deeply grateful to everyone who contributed in any way to the realization of this research.

I would first like to thank my supervisor Dr. Ryan Graham who, for the last few years, has advised and guided me as I sought to make an impact in the world with my research. Your patience and support over the years has not only made this project possible but has fueled my desire to push the current boundaries of knowledge through research. I could not have asked for a better supervisor throughout this journey and for that I want to say thank you.

I would also like to acknowledge Dr. Matthew Mavor's help and support over the course of my studies. This thesis would not have been possible without you. I will ensure the time and effort you spent helping me grow as a researcher is not in vain. You can count this as a first step towards expressing my gratitude for your support.

I would like to thank my advisory committee, Dr. Julie Nantel and Dr. Martin Bilodeau, for taking time out of their schedules to help me through each milestone of my degree. Your patience and support have allowed me to fulfill a project I am proud of.

Every member of the movement biomechanics and analytics laboratory have helped me get to where I am in some way. Allison, Annagh, Camille, Chris, Gwyneth, Heather, Isabel, Jessica, Kristen, Mike, Mohammad, Reza, Victor, Xiong, and Zeeshan, you have all played a part in the researcher I am today.

Je voudrais remercier ma famille : Frédéric, Laurence, Aurelia, Laetitia, et Maxime, pour toutes les heures passées à m'écouter parler de biomécanique et de semelles intelligentes.

Finally, I would like to thank my partner Émilie who has motivated me to reach my full potential and been my guiding light in hard times. I love you beyond compare.

To everyone I mentioned, and the countless other people that have supported me along the way, I just want to say thank you.

List of Tables

Table 5.1 Participant description.	31
Table 6.1 Mean of instrumented insole derived variability and stability metrics as well as inertial measurement unit suit derived foot and trunk stability metrics with standard deviations across 200 strides.	45
Table 6.2 Intraclass correlation coefficients for local dynamic stability values between measurement tools and body segments.	46
Table 6.3 Model summary with correlations and collinearity statistics.	51
Table B.1 Anthropometric measurements for the Xsens MVN Link motion capture suit.	84
Table E.1 List of spatiotemporal variability, raw kinematic variability, and stability metrics.....	87

List of Figures

Figure 2.1 State space reconstruction and calculation of the maximum finite-time Lyapunov exponent.....	14
Figure 5.1 Stride-to-stride spatiotemporal parameters calculated from the instrumented insoles for 200 consecutive strides	39
Figure 5.2 Overlay of the angular velocity output for 200 consecutive normalized right-foot strides with black bars illustrating stride-to-stride dispersion at 90% of the gait cycle.....	40
Figure 6.1 Unstandardized predicted values and studentized residuals.....	48
Figure 6.2 Leverage and influential points	48
Figure 6.3 Normal Q-Q plot of standardized residuals.....	49
Figure 6.4 Regression models fit for trunk local dynamic stability prediction.	50
Figure C.1 Instrumented insole plantar pressure sensor placement.....	85
Figure D.1 Mean and median absolute deviation of yaw (ψ) variability calculation	86

List of Equations

(Eq. 5.1) Pressure threshold.....	35
(Eq. 5.2) Median absolute deviation.....	36
(Eq. 5.3) Stride time.....	37
(Eq. 5.4) Stance time.....	37
(Eq. 5.5) Single support time.....	37
(Eq. 5.6) Double support time.....	37
(Eq. 5.7) Step time.....	37
(Eq. 5.8) Cadence.....	37
(Eq. 5.9) Stride length.....	38
(Eq. 5.10) Stride velocity.....	38
(Eq. 5.11) Euclidian norm.....	40
(Eq. 5.12) State space reconstruction.....	41
(Eq. 5.13) Intraclass correlation coefficient.....	42
(Eq. 5.14) Mean error.....	44
(Eq. 5.15) Root mean square error.....	44
(Eq. 6.1) Multiple linear regression model.....	51

Definition of Terms

3D	Three-dimensional
ANOVA	Analysis of variance
BoS	Base of Support
CoM	Centre of Mass
CoV	Coefficient of variation
DS	Double support
ICC	Intraclass correlation coefficient
IMU	Inertial measurement unit
LDS	Local dynamic stability
MAD	Median absolute deviation
MLR	Multiple linear regression
OMV	Optimal movement variability
PWS	Preferred walking speed
R²	Coefficient of determination
RMSE	Root mean square error
SD	Standard deviation
SLR	Simple linear regression
SOMC	Stereophotogrammetric optical motion capture
SS	Single support
STV	Stride time variability
λ_{\max}	Maximum Lyapunov exponent

Abstract

Gait assessments can help identify individuals at an elevated risk of falling. Gait variability and local dynamic stability (LDS) are considered the most valid measures to assess gait stability and predict gait-related falls. Specifically, LDS of the trunk is most often used to assess gait stability given its important contribution to the centre of mass and the ability to discriminate between fallers and non-fallers using its kinematics. Reliable wearable sensors can be implemented in real-world gait assessments to actively screen for fall risk. Instrumented insoles are an example of unobtrusive wearable technology that can perform accurate gait assessments in real-world settings; however, they have not been validated for gait stability assessments, and cannot directly measure trunk LDS. The purpose of this thesis was to develop a framework to estimate gait stability using instrumented insoles. Fifteen participants were recruited to walk on a treadmill for seven minutes at their preferred walking speed while wearing instrumented insoles and a full-body inertial measurement unit suit. The reliability of foot LDS calculated from instrumented insole data was evaluated against the inertial measurement unit suit using intraclass correlation coefficients. Trunk LDS, measured via the IMU suit, was then predicted by applying linear regressions to the insole-derived metrics. A simple linear regression was used to establish the base amount of variance in trunk LDS that could be explained by foot LDS. Subsequently, a multiple linear regression model consisting of the standard deviation of stride time, standard deviation of double support time, mean single support time, mean yaw variability, and median absolute deviation of yaw variability was used to estimate trunk LDS. Results show that instrumented insoles can reliably measure foot LDS ($ICC_{3,1} = 0.860$). Moreover, the multiple linear regression explained 47.7% more variance than the simple linear regression (adjusted R^2 of 0.845 versus 0.368). This thesis demonstrates that instrumented insoles are an appropriate measurement tool for foot stability and that they can be used to predict trunk LDS with good accuracy during gait.

Chapter 1: Introduction

Gait is a fundamental function of life. Individuals with impaired gait patterns report a loss of mobility, which leads to a loss of personal freedom (Pirker & Katzenschlager, 2017), an increased risk of falling, and, thus, a decreased quality of life (Hulleck et al., 2022; Pirker & Katzenschlager, 2017). Moreover, falls result in a costly burden for the medical system, and lead to an increased prevalence of health problems, especially in older adults (Hamacher et al., 2011; Phelan et al., 2015). By analyzing gait patterns, meaningful information can be gathered regarding an individual's health status (e.g., neurological, musculoskeletal, cardiovascular, and/or metabolic health; Hulleck et al., 2022). Clinicians most commonly analyze gait using mere observation for its simplicity, availability, and low-cost (Hulleck et al., 2022). However, the validity and reliability of observational gait analysis is in question (Ferrarello et al., 2013). Quantitative instruments, such as motion capture technologies, can be used to perform objective gait assessments that can provide insights into gait impairments. Specifically, clinicians and researchers can employ instrumented gait analysis to identify individuals at increased risk of falls, given that gait is the activity of daily life during which falls most often occur (Mertz et al., 2010).

To quantify fall risk, measures of gait stability have been developed. In the present thesis, a stable gait is defined as one that does not lead to a fall following a perturbation (Bruijn et al., 2013). Perturbations are defined as external or unplanned internal forces/moments acting on the system (Bruijn et al., 2013). Various measures of gait stability have been proposed, such as the maximum finite-time Lyapunov exponent (λ_{\max}), maximum Floquet multiplier, long-range correlations, and variability measures. Of the current measures of gait stability, variability measures and λ_{\max} are considered to have the best validity to assess dynamic gait stability (Bruijn et al., 2013), and the combination of variability measures and λ_{\max} has proven to best predict a history of falling in elderly populations (Toebe et al., 2012). Therefore, this thesis will focus on

variability measures and λ_{\max} , as their inclusion in gait assessments may provide the most meaningful biomechanical insights into an individual's risk of falling.

In the context of gait, variability refers to the stride-to-stride fluctuation of a given gait parameter (e.g., stride length, stride time, cadence). Gait variability is typically measured using linear statistical measures (e.g., standard deviation, coefficient of variation, median absolute deviation) to quantify the variation in a gait parameter. Measures of gait variability have been used to successfully predict fall risk through various gait parameters (e.g., stride time (Moon et al., 2015), stance time (Brach et al., 2007), swing time (Verghese et al., 2009), double support phase (Callisaya et al., 2011; Verghese et al., 2009), stride length (Verghese et al., 2009), and step length (Callisaya et al., 2011)). However, the relationship between gait variability and fall risk is ambiguous, as both low and high gait variability have been observed in fallers and non-fallers (Beauchet et al., 2007, 2009; Brach et al., 2005; Hausdorff et al., 2001; Stergiou & Decker, 2011). Therefore, a more in-depth understanding of the relationship between variability measures and gait stability would improve the meaningfulness of gait assessments.

Local dynamic stability (LDS) is defined as the ability to attenuate the effects of infinitesimally small perturbations (Toebe et al., 2012). In essence, LDS is a measure of how quickly a system returns to its original state following a perturbation. LDS is measured through λ_{\max} , which quantifies the average logarithmic rate of divergence or convergence of neighbouring trajectories (Rosenstein et al., 1993). LDS calculations can be used as part of gait assessments to investigate the effect of a variable on gait stability. For instance, LDS can be used to differentiate between fallers and non-fallers in a healthy elderly population (Lockhart & Liu, 2008). When measuring LDS, it is preferable to use the kinematics of the trunk segment as it is the greatest contributor to centre of mass position. Moreover, the trunk is the body's most sensitive marker of

gait impairments, possibly because the nervous system prioritizes the stability of the trunk over that of appendicular segments (Kang & Dingwell, 2009). Consequently, trunk LDS is commonly measured during gait assessments to quantify whole-body stability.

Gait assessments are typically conducted in controlled environments, such as laboratories. In laboratory environments, state-of-the-art equipment, such as stereophotogrammetric optoelectronic motion capture (SOMC) systems, can be used to measure key gait variables; yielding accurate and reliable gait assessments (Merriaux et al., 2017). However, SOMC systems are costly, labour intensive, and restrict the available capture volume (Subramaniam et al., 2022). While controlled gait assessments provide useful information about an individual's gait pattern, they do not reflect the "true" functional gait performance of the individual (Shah et al., 2020). Real-world gait assessments and monitoring provide clinicians with valuable insights into the functional gait performance of patients rather than the optimal performance usually observed in controlled environments (Shah et al., 2020). To conduct gait assessments in real-world settings, wearable sensors are required. To date, numerous wearable technologies have been implemented for gait assessments (e.g., inertial measurement units (IMUs), accelerometers, shoe insoles, and electromyography sensors; Hulleck et al., 2022). Specifically, IMUs are small portable sensors that contain a triaxial accelerometer, gyroscope, and magnetometer that have been successfully used for gait stability analysis (Bailey et al., 2021; Bruijn, Kate, et al., 2010). However, one study found that IMUs are unreliable for gait event detection (e.g., heel strike and toe off), which leads to errors in individual stride values and stride-to-stride variability measurements (Rantalainen et al., 2019). Consequently, a wearable monitoring device capable of accurately identifying gait events to segment a walking bout would improve the precision of gait assessments.

Instrumented insoles are unobtrusive wearable devices that can combine multiple types of sensors, most commonly IMUs and plantar pressure sensors, into an individual's footwear (Subramaniam et al., 2022). The implementation of plantar pressure sensors within the insoles enables the accurate segmentation of walking bouts outside of laboratory settings (Braun et al., 2015; Catalfamo et al., 2008; Chatzaki et al., 2021). Moreover, the IMU embedded in the insole allows the measurement of inertial-driven measures (e.g., LDS, kinematic variability). Since the instrumented insoles are designed to securely fit within a shoe, it can reduce inter-session measurement errors caused by sensor placement variability and are a promising wearable solution for gait assessments (Subramaniam et al., 2022). However, little work has been done to assess fall risk using instrumented insoles. While instrumented insoles are practical for conducting gait assessments in real-world settings, they do not directly measure trunk LDS. Consequently, the present thesis aims to develop a method to estimate trunk LDS from instrumented insole-derived stability and variability metrics. It is hypothesized that the best trunk LDS predictions will be achieved from a combination of foot LDS, kinematic variability metrics, and/or spatiotemporal variability metrics.

Chapter 2: Literature Review

2.1 Falls

In Canada, it is expected that by 2068 more than one in four people will be considered an older adult (> 65 years of age), and the population over 85 years of age will triple (Statistics Canada, 2022). Health concerns arise with an aging population. Notably, falls are a major concern since one in three older adults experiences at least one fall per year in Canada, which accounts for 85% of hospitalization-causing injuries (Pearson et al., 2014). Falls are detrimental to quality of life as they can result in injuries, fear of falling, and decrements in physical, psycho-social, and functional abilities (Vaapio et al., 2009). Consequently, falls lead to a loss of personal freedom (Pirker & Katzenschlager, 2017) and place a large financial burden on the medical system (Hamacher et al., 2011; Heinrich et al., 2010)

Falls are defined as “*An unexpected event in which participants come to rest on the ground floor, or lower level*” (Lamb et al., 2005). Falls are multifaceted in nature, with 156 risk factors identified within the elderly population (Bloch et al., 2010, 2013). By identifying individuals at increased risk of falling, early preventative measures can be implemented. Since falls most commonly occur during some form of locomotion in older adults (Berg et al., 1997; Faulkner et al., 2005; Mertz et al., 2010), researchers and clinicians often perform gait analyses to better understand fall risk.

2.2 Gait

Gait is a fundamental function of life that enables individuals to move forward by producing rhythmic, alternating leg movements while maintaining an upright balance (Moen-Nilssen, 1998). Although seemingly simple, gait requires a complex series of coordinated actions of the neuromusculoskeletal system to allow people to move throughout their environment. A person's gait must be stable and flexible to adapt to changing internal (e.g., mood, fatigue) and

external (e.g., speed, terrain, obstacles) demands while remaining energy efficient. Through gait assessments, information about the health of the underlying locomotor system, such as neurological conditions, musculoskeletal conditions, cardiovascular and metabolic diseases, and age-related physiological deterioration can be revealed (Hulleck et al., 2022). However, gait performance can be impacted, either positively or negatively, by numerous factors including health status (Lord & Rochester, 2005; Middleton et al., 2015; Pirker & Katzenschlager, 2017), cognitive status (Amboni et al., 2013; Duran-Badillo et al., 2020; Morris et al., 2016), motivation and mental health (Michalak et al., 2009; Nagano et al., 2019), muscle activation patterns (Rosati et al., 2021), motor control (Moe-Nilssen, 1998; Sardoğan et al., 2021), sensory function (Duran-Badillo et al., 2020), equipment (e.g., body-borne military equipment (Brown et al., 2014), shoe flexibility (Cranage et al., 2019), hand held weights (Campaña & Costa, 2017), and the environment (Fukuchi et al., 2018; McArdle et al., 2021; Murray et al., 1985; Nymark et al., 2005; Riley et al., 2007; Song & Hidler, 2008; Terrier & Dériaz, 2011)). By assessing an individual's gait pattern, gait abnormalities and inefficiencies can be identified and, potentially, treated.

A typical gait cycle can be separated into two distinct phases for a single leg: swing and stance. In healthy adults, the swing phase, which is when the foot is off the ground, represents 40% of the gait cycle (Mirelman et al., 2018). The swing phase begins when the toes lose contact with the ground (toe off) and is terminated when the heel contacts the ground (heel strike). The swing phase can be further separated into three sub-phases based on the anteroposterior movement of the center of mass (CoM): behind the base of support (BoS; initial swing), inside the BoS (mid swing), and beyond the BoS (terminal swing; Remelius et al., 2014). During the initial swing, the BoS sharply decreases, which positions the CoM medially and posteriorly relative to the BoS. During the mid swing, the CoM moves towards the medial border of the single-support leg, which makes

up the BoS during the swing phase (Lugade et al., 2011). In terminal swing, the movement of the CoM is in a controlled fall as it moves toward the intended step-landing area where the swing foot must be placed to reestablish the state of equilibrium (Remelius et al., 2014). The greatest separation between the CoM and the BoS, which can be considered as an unstable state, is at the toe-off moment (initial swing) and prior to heel strike (terminal swing; Lugade et al., 2011).

The stance phase, which is when the foot is on the ground, represents 60% of the gait cycle (Mirelman et al., 2018). The stance phase can further be separated into single (40% of the gait cycle) and double support (20% of the gait cycle), where one or both feet are in contact with the ground, respectively (Mirelman et al., 2018). The CoM and BoS interaction during the single-support (SS) phase closely resembles the swing phase since the SS phase represents the same portion of the gait cycle as the swing phase of the contralateral leg (Kharb et al., 2011). The double-support (DS) portion of the gait cycle is considered the most biomechanically stable. During DS, the CoM and the centre of pressure remain within the BoS in both the anteroposterior and mediolateral directions (Lugade et al., 2011). DS refers to two portions of the gait cycle: initial DS, which corresponds to the loading phase from heel-strike to contralateral toe-off, and terminal DS, which corresponds to the pre-swing phase from contralateral heel-strike to toe-off (Kharb et al., 2011). Initial DS is also where the step-to-step transition occurs, resulting in the redirection of the CoM velocity (Umberger, 2010). Terminal DS corresponds to the weight transfer phase as the body weight is shifted onto the contralateral leg, and the body is moved forwards by means of plantarflexion (Kharb et al., 2011). The metabolic cost of the two DS phases represents 27% of the total cost of a gait cycle, with initial DS costing three times more than terminal DS (Umberger, 2010). However, when considering the step-to-step transition portion of the gait cycle as initiating and terminating four percent beyond initial DS, the cost of the step-to-step transition alone

increases to 37% (Umberger, 2010). DS is found to have high metabolic cost as it is the phase of the gait cycle where shock absorption, limb loading transfer, propulsion, and CoM velocity redirection occurs (Umberger, 2010). The high metabolic activity suggests high muscle recruitment is required by the locomotor system during DS to perform the above tasks while maintaining or enhance gait stability.

Each phase of the gait cycle contributes to moving forward while maintaining an upright posture through the coordinated movements of the trunk and limbs. The complex interaction between the CoM and the BoS throughout the gait cycle leads to a motion that is repeatedly shifting from a stable position to an unstable position (i.e., CoM moves from inside to outside the BoS; Remelius et al., 2014; Winter, 1995). Through gait assessments, an individual's gait stability can be measured and be used to quantify fall risk.

2.2.1 Gait Stability

Stability is the sensitivity of a dynamic system to perturbations, either finite (i.e., global stability) or infinitesimal (i.e., local stability; Dingwell et al., 2001). Perturbations are described as external (e.g., uneven surfaces) or unplanned internal (e.g., neuromuscular noise) forces or moments acting on the system (Bruijn et al., 2013). In the context of gait analysis, stability can be defined as a gait pattern that does not lead to a fall following a perturbation. If no attenuation occurs following a perturbation, the state of the system deviates from the planned walking trajectory, which can lead to a fall (Bruijn et al., 2013).

Three criteria describing a stable gait have been outlined by Bruijn and colleagues (2013): 1) being able to limit or recover from the infinitesimally small perturbations that occur at each stride (e.g., neuromuscular noise), 2) being able to recover from large perturbations (e.g., slips), and 3) the perturbations need to remain within the recoverable limits of the system. Consequently,

all three criteria should be considered and measured to fully evaluate an individual's gait stability. However, only criterion one, which is representative of an individual's neuromuscular capacity, can be assessed during steady-state walking (Bruijn et al., 2013). This is because the assessment of criteria two and three require perturbations, representative in type and magnitude of those encountered in daily life, to be artificially introduced during a walking trial in a laboratory setting (Bruijn et al., 2013). It is important to note that these criteria are partially independent; an individual may be able to handle small perturbations (criterion 1) but fail to recover from large perturbations (criterion 2; Bruijn et al., 2013). Numerous measures of gait stability, which target the above criteria, have been developed to quantify one's ability to recover from perturbations (e.g., maximum finite-time Lyapunov exponent, maximum Floquet multiplier, gait sensitivity norm, and extrapolated centre of mass).

2.2.2 Measures of Gait Stability

Gait stability metrics can be quantified through stability indices, which originate from mechanical system analysis, and variability indices, which are more statistical in nature (Bisi et al., 2014). Stability indices (e.g., maximum finite-time Lyapunov exponent (λ_{\max}), maximum Floquet multiplier, recurrence quantification analysis, and multiscale entropy) require an assumption about the systems governing gait control: either gait is strictly periodic (e.g., Floquet multiplier) or has aperiodic fractal-like fluctuations (e.g., λ_{\max} ; Dingwell & Kang, 2007). Stability indices can define how systems respond to small perturbations either in real-time (e.g., λ_{\max}) or from one cycle to the next (e.g., Floquet multiplier; Dingwell & Kang, 2007). Conversely, variability indices (e.g., stride-time variability, coefficient of variation, inter-quartile range, harmonic ratio) are thought to arise from noise in the neuromuscular system or the environment (Hamacher et al., 2011). Low variability values indicate a rigid gait pattern that is unaffected by perturbations, either global or infinitesimally small, whereas high variability values indicate less

effective error corrections from the neuromuscular system following a perturbation (Stergiou et al., 2006). High variability values represent an increased fall risk as the increased noise in the gait pattern can bring an individual's dynamic state closer to their limits of stability (Hamacher et al., 2011). The distinction between variability and stability indices is necessary. Although both can be used to predict fall risk, only stability indices directly quantify how the locomotor system responds to perturbations (Dingwell & Cusumano, 2000; Hamacher et al., 2011).

Bruijn and colleagues (2013) describe another gait stability metric classification method by separating measures based on their theoretical origins: dynamical systems theory (i.e., λ_{\max} , Floquet multiplier, variability measures, and long-range correlations) and biomechanics (i.e., extrapolated CoM, stabilizing and destabilizing forces, and foot placement estimator). They also classify the measures of gait stability based on their criteria for a stable gait: the ability to recover from small perturbations (i.e., λ_{\max} , maximum Floquet multiplier, variability measures, long-range correlations, extrapolated CoM, and stabilizing and destabilizing forces), the ability to recover from large perturbations (i.e., gait sensitivity norm, extrapolated CoM, and foot placement estimator), and the maximal perturbation an individual can handle (Bruijn et al., 2013). Bruijn and colleagues (2013) assessed the literature surrounding each measure to comment on the required calculations, each measure's ability to predict the probability of falling, and the validity of the stability metrics. They concluded that the validity of variability measures and the short-term λ_{\max} are best supported by literature to assess dynamic gait stability (Bruijn et al., 2013). However, when considering the effectiveness of gait stability measures on fall prediction, it was found that stride-to-stride variability has a stronger association with fall history than gait instability, measured through the short-term λ_{\max} (Toebe et al., 2012). Nonetheless, the combination of both variability metrics and λ_{\max} in a multivariate logistic regression analysis yielded the best model fit to predict

past falls (Toebe et al., 2012). These findings indicate that fall prediction is improved by the concurrent analysis of gait variability and stability measures rather than investigating them independently.

2.2.2.1 Variability Metrics

Even in the most controlled environments, gait patterns fluctuate from stride-to-stride, typically defined as gait variability. Gait variability is observed in the gait patterns of both healthy individuals (Callisaya et al., 2011; Stergiou et al., 2006; Stergiou & Decker, 2011; Terrier & Reynard, 2015) and individuals affected by pathological conditions (e.g., multiple sclerosis (Socie & Sosnoff, 2013), Parkinson's (Schmitt et al., 2020), and Huntington's (Gaßner et al., 2020)). Variability is traditionally believed to stem from noise in the neuromuscular system that causes random variance in the gait pattern, such that increased variability in the gait pattern reflects poorer gait stability. However, optimal movement variability (OMV) theory suggests an inverted-U shape relationship between variability and stability, indicating an optimal variability point (Stergiou et al., 2006). Although gait variability has been identified in numerous gait variables using various metrics, there is a lack of consensus regarding which variability measure best predicts fall risk.

The presence of variability in a repetitive motor task instigated the development of theories to explain its origins. Traditional variability theories (e.g., uncontrolled manifold hypothesis, dynamical systems theory) suggest a negative linear relationship between motor learning and variability, such that the magnitude of variability decreases as motor learning occurs (Stergiou & Decker, 2011). Alternatively, the OMV theory proposed by Stergiou and colleagues (2006) suggests that, for more mature motor skills, healthy individuals have an optimal amount of variability that reflects the adaptability of an underlying motor control system. When the magnitude of variability diverges from its optimal point, it can yield a noisy and unpredictable or

rigid and predictable system (Stergiou et al., 2006). Therefore, both increases and decreases in gait variability can lead to decreased motor performance. With respect to gait stability and fall risk research, the OMV theory provides an explanation for the ambiguity in results found in the literature, as both low and high gait variability has been observed in fallers and non-fallers (Beauchet et al., 2007, 2009; Brach et al., 2005; Hausdorff et al., 2001; Stergiou & Decker, 2011).

Gait variability is often quantified using descriptive statistical measures, primarily the standard deviation of a signal or a variable (Bruijn et al., 2013). However, Chau and colleagues (2005) found that using the median absolute deviation (MAD) is more statistically stable, with a breakdown point of 0.5 (compared to 0 for standard deviation). Breaking points indicate that an estimator will remain stable until the outliers represent a given proportion of a sample size (Chau et al., 2005). Therefore, MAD is less sensitive to the influence of outliers or noisy data than standard deviation, as it will remain stable until outliers represent 50% of the sample size. To accurately quantify gait variability, large amounts of continuous strides are required. Specifically, spatiotemporal variability requires 200 strides for accurate values (Owings & Grabiner, 2003).

Gait variability is associated with fall history (Toebes et al., 2012) and can help predict future falls within elderly (Callisaya et al., 2011; Hausdorff et al., 2001; Maki, 1997; Verghese et al., 2009) and pathological populations (Ma et al., 2022; Moon et al., 2015). Although positive correlations between fall risk and gait variability exist for various gait parameters (e.g., stride time (Moon et al., 2015), stance time (Brach et al., 2007), swing time (Verghese et al., 2009), double support phase (Callisaya et al., 2011; Verghese et al., 2009), stride length (Verghese et al., 2009), step length (Callisaya et al., 2011), step width (Brach et al., 2005; Hausdorff, 2005; Maki, 1997), and trunk acceleration (Moe-Nilssen & Helbostad, 2005)), there is a lack of consensus regarding which gait variability measure best predicts fall risk. Moreover, variability metrics are generally

considered independent of one another, meaning that the effect of one parameter's variability on another is often neglected. Consequently, exhaustive analyses that consider all gait variability metrics may provide greater insights into the association between gait variability and fall risk than targeted analyses using single variability measures.

2.2.2.2 The Maximum Finite-Time Lyapunov Exponent

In biomechanical research, the maximum finite-time Lyapunov exponent is used to quantify LDS, which is defined as the ability to attenuate the effects of infinitesimally small perturbations (Toebe et al., 2012). λ_{\max} is based on Lyapunov's theory of dynamic stability, which assesses the sensitivity of a mechanical system to small perturbations (Lyapunov, 1992) and represents the average logarithmic rate of divergence of infinitesimally close trajectories in a state space (Bruijn et al., 2009b). Higher values of λ_{\max} represents a more chaotic system, whereas lower values represent a more stable system (Rosenstein et al., 1993). Over time, recommendations have been made to accurately measure λ_{\max} with considerations for both study design and analysis.

λ_{\max} calculations are done using two main algorithms: the one presented by Wolf and colleagues (1985) and the one presented by Rosenstein and colleagues (1993). Both algorithms are based upon the definition of λ_{\max} from dynamical systems theory as they calculate the average logarithmic rate of divergence between two neighbouring trajectories in a state space (Bruijn et al., 2013). A state space is a representation of all states (i.e., configurations/behaviours) of a system, where each state corresponds to a unique time-point in the state space (Bruijn et al., 2013; Kang & Dingwell, 2006). For repetitive movements, the state space will generally exhibit the structure of an attractor (i.e., the average movement pattern towards which the system tends to converge; Dingwell et al., 2007). The Wolf algorithm calculates λ_{\max} by identifying the nearest neighbour for data points along a single reference trajectory. However, the Wolf algorithm is

considered unreliable for small data sets because it does not use all available data but rather follows a single nearest neighbour that is replaced when its separation from the reference trajectory passes a certain limit (Cignetti et al., 2012; Rosenstein et al., 1993). In contrast, Rosenstein’s algorithm does not replace a trajectory but rather takes advantage of all attractor data points in the state space, which removes approximation in the results (Rosenstein et al., 1993). To calculate λ_{\max} using the Rosenstein algorithm, an n -dimensional state-space is constructed from the experimental data, where n is the number of state variables (Gates & Dingwell, 2009; Raffalt et al., 2020; Rosenstein et al., 1993). From the state space, the log can be taken from the expansion/contraction of the Euclidean distance between the nearest neighbouring data points (Bruijn et al., 2013), and the slope of the average divergence curve is taken to estimate LDS (Rosenstein et al., 1993). The procedure to calculate λ_{\max} is depicted below in Figure 2.2.1.

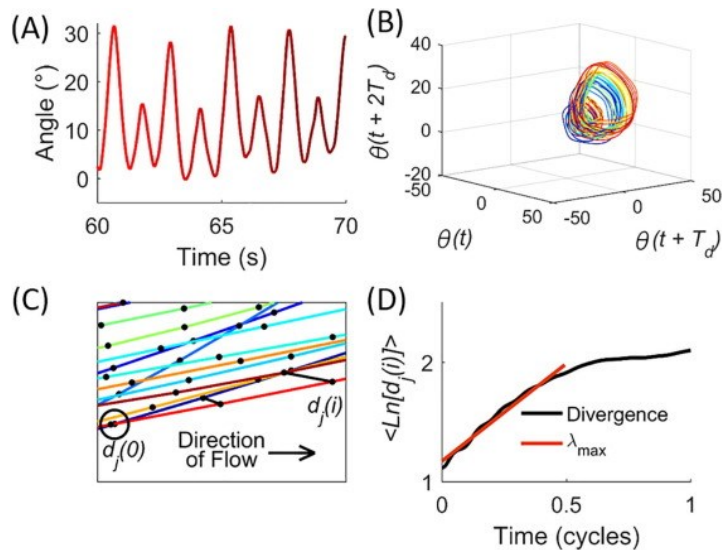


Figure 2.1 State space reconstruction and calculation of the maximum finite-time Lyapunov exponent. (A) The zoomed-in original 3D angular data for a repetitive task. (B) Reconstruction of a 3D state space. (C) Expanded view of a local region on the reconstructed attractor illustrating the divergence of nearest neighbouring trajectories following an infinitesimally small perturbation. (D) Average logarithmic rate of divergence of all nearest neighbour trajectories. From (Beange et al., 2019).

Considerations must be taken when calculating λ_{\max} , mainly regarding state space reconstructions. In biomechanical data, the state variables used to reconstruct the state space

typically include displacement, velocity, and/or acceleration in linear and/or angular directions (Gates & Dingwell, 2009). State variables can also be constructed with delay-embedded dimensions, which are constructed using time-delayed versions of an observed scalar quantity (Raffalt et al., 2020). Time-delay embedding is used to reconstruct the dynamics of a system while preserving the nonlinear relationships of the time-series data to represent the original system (Kennel et al., 1992). Further, using time-delayed embedded dimensions can aid in simplifying data collection protocols by reducing the number of unique variables required and, in turn, avoiding data that is more prone to error (Gates & Dingwell, 2009). The proper selection of the embedding dimension, to avoid over- or under-estimating the required embedding dimension, can be done using Global False Nearest Neighbour analysis (Kennel et al., 1992). The Global False Nearest Neighbour analysis examines how the number of neighbours of a point change with increasing embedding dimensions; such that increasing from dimension m to $m + 1$ yields a negligible number of false neighbours (Krakovská et al., 2015). Time-delay selection is also important for proper state space reconstruction to limit dependence between time-delayed copies. To identify the optimal time-delay, the average Mutual Information function, which measures the general dependence between two variables, can be used (Fraser & Swinney, 1986). It was first believed that describing a system with every degree of freedom was advantageous, leading to 12-dimensional state spaces consisting of 3D translations and 3D rotations and their time derivatives (Kang & Dingwell, 2006, 2009). However, it was found that redundant information (e.g., including all angles and angular velocities of a joint) could negatively impact the results (Gates & Dingwell, 2009). From their analysis of the effect of state space definition on λ_{\max} results, Gates and Dingwell (2009) found that the qualitative trends of λ_{\max} persist regardless of the state space. Therefore, state

space reconstructions from multiple measurable biomechanical state variables, while minimizing redundant information, could yield the most reliable λ_{\max} values (Gates & Dingwell, 2009).

The data time-series length is another important aspect to consider for reliable λ_{\max} values. Specifically, it is important to retain the same number of samples for each participant across conditions, if applicable, as the length of the time-series affects λ_{\max} (Bruijn et al., 2009a) due to the nearest neighbour trajectories becoming increasingly closer together as time increases (Bruijn et al., 2012). Traditionally, measures of λ_{\max} are calculated as the rate of divergence per second. However, during gait, every foot-ground contact can be considered an opportunity for a person to recover from a perturbation. Consequently, it was suggested to express the rate of divergence per gait cycle, rather than per second (Bruijn et al., 2009a, 2012, 2013; Dingwell & Cusumano, 2000). Moreover, λ_{\max} values are found to increase in precision with increasing number of strides included (Bruijn et al., 2009a). As increases in precision appear to plateau after 150 strides, it is recommended to use a minimum of 150 strides to calculate λ_{\max} (Bruijn et al., 2009a).

With respect to stability, positive λ_{\max} values indicate divergence between the neighbouring trajectories (i.e., an unstable system) and negative values indicating convergence of the neighbouring trajectories (i.e., a stable system; Ihlen et al., 2017; Rosenstein et al., 1993). Therefore, higher positive λ_{\max} values are indicative of greater instability. In gait stability analyses, two values of λ_{\max} are often reported: the short-term maximum finite-time Lyapunov exponent (λ_S) and the long-term maximum finite-time Lyapunov exponent (λ_L). λ_L is calculated from 4-10 strides and represents the maximal separation between neighbouring trajectories (Bruijn et al., 2009a, 2009b). It is believed that λ_L quantifies the inherent stability of the system (Su & Dingwell, 2007). However, it was not found to be a valid estimate of someone's probability of falling as it does not reflect the addition of instability in a model (Bruijn et al., 2012; Hak et al., 2012; McAndrew et

al., 2011; Sloot et al., 2011; Su & Dingwell, 2007). Contrastingly, λ_S , which is calculated from 0-0.5 strides, is thought to represent the greatest rate of expansion of any dimension in the state space (Bruijn et al., 2009a, 2009b). Since λ_S can reflect the addition of instability in a model, it is considered a valid measure of someone's risk of falling (Su & Dingwell, 2007).

Local dynamic gait stability quantifies one aspect of gait: the ability to attenuate the effects of infinitesimally small perturbations on the gait pattern (Toebe et al., 2012). Numerous recommendations have been put forth to estimate LDS, including the state variables to use, the number of strides to analyze, and the λ_{\max} value to report. The successful use of LDS to discriminate between fallers and non-fallers (Toebe et al., 2012), renders it a valid method to predict falls (Bruijn et al., 2013). Notably, an individual's gait stability is most often assessed from the kinematics of the trunk segment. The trunk plays an essential role in whole-body movement generation and is a significant contributor to CoM kinematics. Moreover, it is believed that the nervous system prioritizes the stability of the trunk over that of the appendicular segments during locomotion (Kang & Dingwell, 2009). Therefore, measuring trunk LDS can provide meaningful insights into an individual's risk of falling.

2.2.3 Trunk Stability

The human trunk, comprised of the thorax, abdomen, and back regions, contains 33 vertebrae, 24 ribs, and the sternum. To generate the movements of this highly articulated segment, the trunk is synergistically actuated by multiple muscles (e.g., internal obliques, erector spinae, latissimus dorsi). The complexity of the segment necessitates a combination of anticipatory and reactive actions from its actuating muscles to regulate its movements (Ceccato et al., 2009). However, the anatomical complexity of the trunk makes it a versatile segment that can actively

participate in various tasks (Kumar, 2004). Given the trunk's versatility and centrality in the body, it is considered the base of all functional movements (Karthikbabu et al., 2011).

The musculoskeletal components, in combination with the vital organs and adipose tissue, found in the trunk accounts for approximately 47% of the total body mass (Hari Krishnan et al., 2016). To maintain an upright posture during gait, which is dependent on the ability to constrain the CoM within the BoS (Kluger et al., 2014), individuals must control the displacement of their trunks to minimize deviations of the CoM from the BoS. Given the trunk's high contribution to CoM kinematics, in some cases, it is preferable to reduce CoM motions by controlling trunk motions rather than by altering foot placement (Best et al., 2019). For instance, stability can be increased by controlling trunk rotations, which limits the motion of the CoM (Hof, 2007). Further, to support trunk neuromuscular control, healthy adults reduce the trunk's moment of inertia by synchronously and contralaterally moving their upper and lower limbs (Sparrow & Newell, 1994). Notably, trunk LDS is increased with increasing arm swing amplitude, possibly due to the resulting increase in angular momentum (Hill & Nantel, 2019). By controlling the movements of the trunk, the body can remain upright, adjust weight shifting, and perform dynamic postural adjustments to control the velocity and position of the CoM in relation to the BoS (Karthikbabu et al., 2011).

Given the trunk's essential role in whole-body movement and balance, the study of its kinematics, kinetics, and muscle activity has garnered interest relating to its stability, specifically during locomotion. Consequently, the trunk segment is often used to quantify whole-body gait stability and discriminate between fallers and non-fallers through local dynamic stability computations (Bizovska et al., 2018; Ihlen et al., 2016; Rispens et al., 2015; Toebe et al., 2012). Notably, Kang and Dingwell (2009) found that trunk stability is a more sensitive marker of gait impairment than stability measured using lower body segments. Relative to the feet, the trunk's

inertia is significantly greater due to its greater mass, which aids in perturbation attenuation (Kang & Dingwell, 2009). Although its greater inertia makes the trunk a more stable segment than the feet, correcting its motions has a greater metabolic cost (Kang & Dingwell, 2009). For this reason, it is believed that the nervous system prioritizes the stability of the trunk over that of the appendicular segments during locomotion (Kang & Dingwell, 2009). Rather, movements of the appendicular segments play a stabilizing role on the trunk during gait (Ortega et al., 2008) and aid in the recovery from perturbations (Bruijn, Meijer, et al., 2010).

2.3 Motion Capture

In biomechanics, human movement is traditionally measured using stereophotogrammetric optoelectronic motion capture (SOMC) systems. SOMC systems use infrared light emitted from multiple cameras placed around a capture volume to provide accurate three-dimensional (3D) positions of markers placed on the skin (Merriault et al., 2017). SOMC systems are considered the “gold standard” for 3D motion analysis as they have instrument errors below 2 mm (Merriault et al., 2017; Spörri et al., 2016). However, there are some limitations to SOMC systems such as being prone to skin motion artifact (i.e., the movement of markers on the skin relative to the underlying skeletal system; Camomilla et al., 2017; Fuller et al., 1997; Holden et al., 1997; Schwartz et al., 2004), confined to a laboratory setting (Blair, 2019; Subramaniam et al., 2022), costly (Subramaniam et al., 2022), labour-intensive (Blair, 2019), they require trained personnel (Subramaniam et al., 2022), and their accuracy is limited by marker occlusions. As such, numerous motion capture alternatives have been developed and tested over the years such as stereoradiography (Jonsson & Kärrholm, 1994), markerless motion capture (Kanko, Laende, et al., 2021; Kanko, Strutzenberger, et al., 2021; Rammer et al., 2018), and wearable sensors (e.g., inertial measurement units (IMUs); Bailey et al., 2021; Beange et al., 2019; Hamacher et al., 2015; Mavor et al., 2020).

2.3.1 Inertial Measurement Units

There has been a recent push to calculate meaningful gait metrics with wearable sensors. Inertial measurement units (IMUs) are often comprised of a triaxial accelerometer, gyroscope, and magnetometer to measure linear acceleration, angular velocity, and magnetic field strength and direction, respectively (Tao et al., 2012). IMUs can be used to continuously monitor biomarkers, defined as objective indications of medical state observed from outside the patient (Strimbu & Tavel, 2010), using their small, portable, self-contained sensors (Ceren Ates et al., 2022). Consequently, IMUs offer a promising wearable alternative for motion capture outside of laboratory settings. Meaningful variables can be calculated from IMU data by either analyzing the collected signals (e.g., gait event identification (Rantalainen et al., 2019), inertial-based LDS assessment (Bizovska et al., 2018), and gait abnormality assessment (Sekine et al., 2013)) or by applying a sensor fusion algorithm (Caruso et al., 2021; Ligorio et al., 2016).

The simultaneous collection of acceleration, angular velocity, and magnetic field strength and direction, when applicable, can provide a comprehensive measurement of the sensor's motion. Regarding motion capture, IMUs enable the analysis of an individual's kinematics by extracting meaningful information from the sensor's data. One method to extract meaningful information from IMU sensor data is to use sensor fusion algorithms. By combining the data from multiple sensors, sensor fusion algorithms can provide a single measurement that outperforms each sensor individually (Novak & Riener, 2015). In the case of IMUs, sensor fusion algorithms are used to reliably calculate the orientation of the IMU sensor from the accelerometer, gyroscope and/or magnetometer data. The orientation of the sensor allows for the removal of the earth's gravity from the acceleration signal. The IMU's position relative to its initial position can then be estimated through double integration of the gravity-removed acceleration signal (Kok et al., 2017).

IMUs can be used for motion capture and motion analysis as independent sensors, or they can be combined to create a complete system. One such IMU system is the Xsens MVN BIOMECH Link system (Xsens, Enschede, Netherlands), which is the system of interest for this project. The Xsens MVN Link system uses a specific biomechanical model and 17 IMU sensors placed on specific body segments to estimate 3D joint kinematics. The Xsens system has been validated for various tasks inside and outside of laboratory settings including level walking (Ferrari et al., 2009; Laudanski et al., 2013; Zhang et al., 2013), stair ascend/descend (Laudanski et al., 2013), military tasks (Mavor et al., 2020), tennis (Pedro et al., 2021), and kicking (Blair, 2019; Blair et al., 2018). Therefore, the Xsens system can be considered a valid motion capture system for full-body kinematic-based gait analyses.

IMUs display a promising avenue for motion capture in real-world settings, notably for gait assessments. The cost- and labour efficiency gained from IMUs demonstrate the possibility of leveraging the technology to continuously monitor biomarkers. Notably, IMUs have been used to measure LDS (Bailey et al., 2021; Bizovska et al., 2018; Bruijn, Kate, et al., 2010; Hamacher et al., 2015; Ihlen et al., 2016; Kobsar et al., 2020; Jian Liu et al., 2012; Rispens et al., 2015). However, IMU sensors are still prone to skin motion artifact as the sensors are generally affixed to the skin to reflect the motion of the underlying segment (Forner-Cordero et al., 2008). Moreover, IMUs are prone to between-session errors caused by sensor placement variability, which decreases the test-retest reliability of IMU-derived measurements (van Schooten et al., 2013). When evaluating the reliability and validity of IMUs for gait assessments against an SOMC system, Rantalainen and colleagues (2019) found poor validity of spatiotemporal gait variability metrics. They attributed the low validity results to the misidentification of gait events for the IMU system, which resulted in incongruent stride spatiotemporal values between the IMUs and the SOMC.

From the above limitations of IMUs, it becomes apparent that alternative wearable devices may improve real-world gait assessments and monitoring.

2.3.2 Instrumented Insoles

Integrated wearable devices are devices that couple multiple types of sensors for more complex measurements. Such devices include smart watches, fitness bands, posture belts, and instrumented insoles. Specifically, instrumented insoles can contain various sensors including, but not limited to, plantar pressure sensors (range from 3 (Motha et al., 2015) to 280 (Sorrentino et al., 2020)), accelerometers (Choi et al., 2019), gyroscopes (Choi et al., 2019), ultrasound (Mohamed Refai et al., 2019), force (Mohamed Refai et al., 2019; Mustufa et al., 2015), temperature (Mustufa et al., 2015), and IMUs (Chatzaki et al., 2021; Chen et al., 2021; Mohamed Refai et al., 2019; Mustufa et al., 2015; Roth et al., 2018). The most common sensor combination found in an instrumented insole are pressure sensors and IMUs (Subramaniam et al., 2022). The addition of pressure sensors to IMUs within instrumented insoles provides an opportunity to accurately detect gait events (Chatzaki et al., 2021), thus overcoming the limitation of IMUs. Therefore, instrumented insoles are a desirable alternative to conduct valid and reliable gait assessments.

The use of instrumented insoles has been validated for a number of tasks, including balance (Oerbekke et al., 2017), running (Cramer et al., 2022), jumping (Burns et al., 2017; Stöggl & Martiner, 2016), cross-country skiing (Stöggl & Martiner, 2016), and, most importantly to this work, walking (Burns et al., 2017; Cramer et al., 2022; Oerbekke et al., 2017; Stöggl & Martiner, 2016; Van Hooren et al., 2023). Typically, force platforms are used for gait event determination; however, they are restricted to laboratory environments and by the number of force platforms available for continuous gait monitoring (Catalfamo et al., 2008). The plantar pressure sensors available in instrumented insoles enable the accurate segmentation of walking bouts into the phases

of the gait cycle through the identification of gait events outside of laboratory settings (Braun et al., 2015; Catalfamo et al., 2008; Chatzaki et al., 2021). The high accuracy of gait event identification through plantar pressure data suggests that gait assessments conducted with instrumented insoles may be more precise than assessments conducted with IMUs. Moreover, the IMUs integrated within the instrumented insoles enable the estimation of spatial metrics through sensor fusion algorithms (Ligorio et al., 2016) and stability calculations at the feet (Hamacher et al., 2015). Further, the design of instrumented insoles, which require them to fit within the footwear, reduces the placement variability of the sensors relative to the segment. Consequently, instrumented insoles may yield results with less error and noise than IMUs as they allow for less sensor placement variability.

An important consideration when developing wearable technology is the end-user's likelihood of adopting the technology in their daily lives. Although IMU systems provide a promising alternative for daily monitoring of patients outside of the laboratory or clinical settings, it was found that less than 15% of clinicians make use of IMUs in their practice and one-third of consumers of wearable devices stop using their device within six months (Lee et al., 2016; Lin et al., 2019). Consequently, developers should avoid clunky and unfashionable devices to improve the adoption of the device by the public (Lewis & Neider, 2017). Instrumented insoles follow this recommendation as they reside within the shoe, where they remain unnoticed. For the above reasons, instrumented insoles are an interesting alternative for real-life gait assessments. Considering the high prevalence of gait-related falls, gait assessments via instrumented insoles are a potential route for unobtrusive gait stability analysis in real-world settings. However, the reliability of instrumented insoles must first be ascertained, and a framework to predict trunk stability from insole data must be outlined.

2.4 Statistical Analyses

Statistics are an important part of a study. Statistical analyses help researchers identify trends and interpret the data they collected to answer a research question. Statistics can be grouped into two general categories: descriptive statistics (i.e., generate numeric descriptions of the data) and inferential statistics (i.e., make comparisons and draw conclusions from the data; Simpson, 2015). To implement new instruments (e.g., instrumented insoles) for clinical or research purposes, it is important to assess the reliability of measurements against a previously validated system (e.g., Xsens IMU suit). Consequently, statistical measures, such as intraclass correlation coefficients, are needed to quantify the correlation and agreement between systems. Moreover, methods such as linear regressions enable the prediction of measures that cannot be directly measured from other variables (Simpson, 2015). Given the inherent limitation of instrumented insoles to measure trunk stability, linear regression techniques may be advantageous to predict trunk stability from variables measured using the insoles.

2.4.1 Intraclass Correlation Coefficients

Intraclass correlation coefficient (ICC) is an index of the degree of correlation and agreement between measurements (Koo & Li, 2016). ICCs can be interpreted as “*the proportion of variance that is attributable to objects of measurement*” (McGraw & Wong, 1996). ICCs can be used to evaluate the interrater, test-retest, and intra-rater reliability in a dataset, which provides confidence in the measurements (Koo & Li, 2016). To quantify reliability, ICCs require a linear relationship between the variables, similar to Pearson correlations (Jinyuan Liu et al., 2016). However, Pearson correlations solely reflect the correlation between two measures, whereas ICCs reflect both the correlation and the agreement between measurements, making them a better measure of reliability (Koo & Li, 2016).

Various ICC models have been defined based on the “Model”, “Type”, and the “Definition” of the relationship that exists between measurements (Koo & Li, 2016; McGraw & Wong, 1996). The “Model” refers to the one-way/two-way random effects or two-way mixed-effects possibilities and is identified in the first number of the ICC form. A one-way random-effects model, identified by a “1” (i.e., $ICC_{1,1}$ or $ICC_{1,k}$), indicates that each subject has a different set of raters selected at random (Koo & Li, 2016). A two-way random-effects model, identified by a “2” (i.e., $ICC_{2,1}$ or $ICC_{2,k}$), refers to a model where the raters are randomly selected amongst a larger set of raters with similar characteristics (Koo & Li, 2016). A two-way mixed-effects model, identified by a “3” (i.e., $ICC_{3,1}$ or $ICC_{3,k}$), is used if the raters being assessed are the only ones of interest (Koo & Li, 2016).

The “Type” of ICC refers to either single or average measurements and is identified by the second number in the ICC form (McGraw & Wong, 1996). Single measurement ICCs, identified by a “1” (i.e., $ICC_{1,1}$; $ICC_{2,1}$; or $ICC_{3,1}$), are used when the measurements of one rater are defined as the “true” measurement and estimate the correlation between raters (Koo & Li, 2016). Average measurement ICCs, identified by a “k” (i.e., $ICC_{1,k}$; $ICC_{2,k}$; or $ICC_{3,k}$), are used when the desired reliability index should be calculated by taking the average of k raters’ measurements for each subject (Koo & Li, 2016).

The “Definition” of ICC refers to either the absolute agreement or consistency between measurements (McGraw & Wong, 1996). These different definitions only apply to two-way models; one-way models always assess absolute agreement (McGraw & Wong, 1996). Absolute agreement ICCs are used for reliability assessments where the same score is given to each subject by different raters (Koo & Li, 2016). Consistency ICCs are used when a systematic error is expected between the two raters (Koo & Li, 2016).

Once the appropriate form of ICC is selected and the data analyzed, the findings can be interpreted. Currently, there are no accepted standard values for what qualifies as acceptable reliability (Koo & Li, 2016). Using a sample size of 30 and three raters, Koo and Li (2016) suggest the following thresholds: poor: $0 < ICC < 0.5$; moderate: $0.5 < ICC < 0.75$; good: $0.75 < ICC < 0.9$; excellent: $0.9 < ICC$. To properly report ICCs, it is recommended to include the software information, the form of ICC (i.e., model, type, and definition), the ICC estimate, and the 95% confidence interval.

In the context of gait assessment with wearable technology, an evaluation of the agreement between systems must be conducted prior to the implementation of a novel system. The most appropriate ICC form to validate a new system (e.g., instrumented insoles) against a pre-established system (e.g., Xsens suit) for a given measurement (e.g., λ_{max}) is a two-way mixed effect, consistency, single rater ($ICC_{3,1}$). A two-way mixed effect model indicates that the raters included in the analysis are the only raters of interest. Defining the ICC form for consistency between raters reflects the possibility of having a systematic difference between the measures of each system. The single rater type of ICC is used as the pre-established system provides ground-truth values to which the novel system can be compared.

2.4.2 Multiple Linear Regression

Multiple linear regressions (MLRs) are used to find the relationship between multiple predictor variables and one outcome variable. By accounting for multiple predictor variables, the individual associations with the outcome of interest and the interaction between variables can be studied. The outcome of an MLR analysis is a regression equation that represents the relationship between the predictor variables and the outcome variable (Tranmer et al., 2020).

Prior to analyzing the results of an MLR analysis, several assumptions must be met. The first two assumptions are related to the type of data collected during the study: one dependent variable must be measured on a continuous level, and two or more independent variable measures must be collected on a continuous or nominal level (Tranmer et al., 2020). Once ascertained that the analysis is appropriate for the study, six assumptions relating to data fit must be tested: the independence of observation, linear relationship, homoscedasticity of residuals, multicollinearity, and the normal distribution assumption. The independence of observation assumption is tested with the Durbin-Watson test, for which the value must fall between 1.5 and 2.5 (Trunfio et al., 2022). The linearity assumption states that a linear relationship must exist between 1) the dependent variable and each of the independent variables and 2) the dependent variable and the independent variables, collectively. The linearity assumption can be checked via the partial regression plots between each independent variable and the dependent variable (1; Larsen & McCleary, 1972) and via the scatterplot of the studentized residuals and the unstandardized predicted values (2; Trunfio et al., 2022). The assumption of homoscedasticity of residuals, or constant variance across all subjects, is also assessed using the scatterplot of the studentized residuals and the unstandardized predicted values (Tranmer et al., 2020). The data must not show multicollinearity, which occurs when two or more independent variables are highly correlated (Tranmer et al., 2020). In general, it is accepted that the multicollinearity assumption is not violated when the variance inflation factor (VIF) is below 10 (Tranmer et al., 2020). Further, there should be no outliers, leverage points, or highly influential points in the data (Eberly, 2007). Lastly, the residuals must be approximately normally distributed (Tranmer et al., 2020). The normal distribution can be assessed via a percentile-percentile plot, a quantile-quantile plot, and/or a histogram with a superimposed normal curve (Tranmer et al., 2020). Should any assumption be

violated, data transformation techniques can be applied to a data set to meet the assumptions outlined above (Marill, 2004a).

The equation derived from the regression analysis is comprised of the predictor variables and their coefficients, as well as a constant term. The linear nature of the equation creates a flat plane in n dimensions (Marill, 2004b). To determine the equation that best fits the data, the least-squares method is used. The least squared method will identify the equation that minimizes the squared sum of the residuals, which is the difference between the actual and the predicted outcome value (Marill, 2004b). To assess the fit of the regression model, the coefficient of determination, R^2 , is calculated. R^2 quantifies the proportion of the variation in the outcome variable that can be explained by the predictor variables (Marill, 2004b). The adjusted R^2 value is often reported alongside the R^2 value in regression analyses (Tranmer et al., 2020). Compared to the R^2 value, which can only increase as more predictor variables are added to the regression model, the adjusted R^2 penalizes the inclusion of unnecessary variables in the model (Ratner, 2009). Furthermore, the adjusted R^2 value adjusts for the sample size and number of predictor variables in the regression model (Ratner, 2009). To test the significance of the model and indicate if the MLR model explains some of the variance in the outcome variable, an analysis of variance (ANOVA) for regression is used (Marill, 2004b).

The statistical power of an MLR analysis, which is the probability of rejecting the null hypothesis when the null hypothesis is false, is based on the magnitude of the effect and the degree of uncertainty in the results (Marill, 2004b). Statistical power can be increased by increasing the magnitude of the effect or by decreasing the uncertainty in the results (Marill, 2004b). When possible, collecting more data will increase power and decrease uncertainty in the results (Marill, 2004b). Alternatively, when the sample size, n , is fixed, the statistical power can be increased by

including more noncollinear predictor variables, decreasing uncertainty. Moreover, sample size will determine the maximum number of predictor variables that can be included in a linear regression model through the subject-to-variable ratio. Various recommendations exist regarding the subject-to-variable ratio required for accurate predictions in regression models. Notably, when investigating the subject-to-variable ratio required for linear regressions, Austin and Steyerberg (2015) found that a ratio of two is sufficient for regression coefficient, standard error, and confidence interval estimations. Consequently, MLR analyses should use a minimal subject-to-variable ratio of two. However, Austin and Steyerberg (2015) also highlight the need to report the adjusted R^2 value when working with low subject-to-variable ratios as the estimated R^2 statistic could be artificially inflated. An inflated R^2 could affect the generalizability of the model as it would decrease its prediction accuracy when applied to the data of new subjects (Austin & Steyerberg, 2015). Although no guidelines are provided to classify sample sizes, samples that yield subject-to-variable ratios near two can be considered small and require the use of the adjusted R^2 .

2.5 Summary

Falls place a costly burden on medical systems and a decrease in quality of life. Instrumented gait assessments can be used to identify individuals at increased fall risk. Specifically, variability measures and local dynamic stability are considered valid measures to predict falls. Gait stability is often measured from trunk kinematics as it plays an important role in centre of mass position and has been successfully used to discriminate between fallers and non-fallers. However, measuring trunk stability in real-world settings from IMUs is impractical and prone to errors in gait event detection as well as between-day measurements due to sensor placement variability. Instrumented insoles are a promising alternative to conducting gait assessments as they can accurately identify gait events, and their placement inside the footwear minimizes sensor placement errors.

Chapter 3: Purpose

Estimate trunk local dynamic gait stability during treadmill walking using instrumented insoles (Neurogait 3.0, Salted, South Korea) containing an accelerometer, a gyroscope, and six pressure sensors. Trunk local dynamic stability will be directly calculated via trunk data obtained from a whole-body inertial measurement unit suit (MVN Link, Xsens, Netherlands) and predicted through a multiple regression model using feet LDS, kinematic variability, and spatiotemporal variability as potential predictors.

Chapter 4: Hypothesis

Instrumented insoles can measure key metrics to enable gait analysis without the need for costly, constraining, and time-consuming motion capture systems (Chatzaki et al., 2021; Subramaniam et al., 2022). λ_{\max} and variability measures have the most support from the literature for estimating stability (Bruijn et al., 2013). Further, the combination of λ_{\max} and variability measures can predict fall history better than when analyzed individually (Toebe et al., 2012). Therefore, it is hypothesized that reliable LDS values will be obtained using data from the instrumented insoles and that trunk LDS estimations will be improved by the addition of stride-to-stride variability measures from foot kinematic and spatiotemporal variables in the multiple regression model.

Chapter 5: Methods

5.1 Participants

16 healthy individuals (9 males and 7 females) over the age of 18 were recruited through word of mouth from the Ottawa community. An individual was considered healthy if they had no musculoskeletal disorders (e.g., sprains, strains, and fractures) that would limit their ability to adopt a natural gait pattern at the time of the data collection. Individuals were excluded from study participation if they were experiencing a musculoskeletal disorder at the time of the study, if a clinician had advised them against prolonged walking, or if their age fell outside of the age limits. Age limits were set to the age range for adults (i.e., 18 to 65 years of age (Kang & Dingwell, 2008)). Older adults were not included as there are known differences in LDS and variability values in the older adult population relative to the adult population.

Data were analyzed for 15 out of the 16 participants. The data from one male in the 20-25 age group were excluded because instrumented insole gait detection failed to identify all gait events from the data due to mid-foot/forefoot landing patterns driven by past ankle injuries. Therefore, the metrics calculated from their data were deemed unreliable.

Table 5.1 Participant description.

Age groups (years)	Number of participants	Height (m)	Leg length (m)	PWS (km/h)
		Mean (SD)	Mean (SD)	Mean (SD)
20-25	6 (3 M, 3 F)	1.76 (0.07)	0.91 (0.04)	4.43 (0.95)
25-30	4 (1 M, 3 F)	1.74 (0.08)	0.90 (0.06)	4.83 (0.45)
30-35	2 (2 M, 0 F)	1.84 (0.07)	0.95 (0.02)	4.99 (0.92)
35-40	2 (1 M, 1 F)	1.77 (0.10)	0.93 (0.02)	4.43 (0.11)
55-60	1 (1 M, 0 F)	1.81 (N/A)	0.97 (N/A)	4.35 (N/A)
Total	15 (8 M, 7 F)	1.76 (0.07)	0.92 (0.04)	4.59 (0.69)

Abbreviations: SD = Standard deviation; m = meters; km/h = kilometers per hour; PWS = Preferred walking speed; M = Male; F = Female.

5.2 Participant Preparation

Upon their arrival to the laboratory, participants were provided with a paper copy of the consent form to read (Appendix A), and the project overview/data collection protocol was verbally explained to them in full to ensure their informed consent was provided. The study was approved by the University of Ottawa research ethics board (Ethics file number: H-11-21-7565). The participant's anthropometric data were then recorded: body height, foot size, arm span, wrist span, elbow span, ankle height, hip height, hip width, knee height, shoulder height, and shoulder width. The anthropometric values were required for the initialization and scaling of the Xsens biomechanical model. Descriptions of the measurements can be found in Appendix B.

The participants were then asked to change into athletic shorts and a custom Lycra[®] T-shirt designed by the Xsens company (Link shirt, Xsens, Netherlands) with Velcro[®] locations to host the shoulder, and sternum sensors, as well as a battery pack and an on-board computer. Seventeen IMU sensors were then placed and secured on the participants: 2 x shoulder, 2 x upper arms, 2 x forearms, 2 x hands, 1 x pelvis, 1 x head, 1 x thorax, 2 x thighs, 2 x shanks, and 2 x feet. Neoprene straps with Velcro[®] were used to secure the arm, forearm, pelvis, thigh, and shank sensors ($n = 9$). The participants were also provided with gloves designed to hold the hand IMU sensors and a headband, which held the head IMU sensor. The Xsens IMU suit uses a right-handed coordinate system such that x represents acceleration in the anteroposterior direction (anterior is positive), y represents acceleration in the mediolateral direction (left is positive), and z represents acceleration in the vertical direction (superior is positive). The IMU suit was used as the ground-truth for the participants' full-body movements as it has previously been validated for full-body motion capture (Bailey et al., 2021; Laudanski et al., 2013; Mavor et al., 2020; Pedro et al., 2021; Zhang et al., 2013), and, most importantly for the proposed thesis project, for local dynamic stability assessments (Longo et al., 2018; Punt et al., 2015; Saber-Sheikh et al., 2010). Based on the

participant's shoe size, the appropriately sized instrumented insole pair was selected and placed inside the participant's shoes. Each instrumented insole contained six pressure sensors (Appendix C), a triaxial accelerometer set at a maximal linear acceleration of 8 g's, and a triaxial gyroscope with a maximal angular velocity of 2000 degrees per second. The instrumented insoles follow a left-handed coordinate system where x represents accelerations in the mediolateral direction (left is positive), y represents accelerations in the antero-posterior direction (anterior is positive), and z represents accelerations in the vertical direction (superior is positive). The positive angular velocities around each axis also correspond to a left-handed coordinate system.

Prior to data collection, two calibration procedures, one per motion capture system, were performed to ensure the accuracy of the collected data. The instrumented insoles, which were controlled by a laboratory owned smartphone (iPhone 12, Apple, USA), were calibrated by lifting the left foot off the ground for three seconds followed by the right foot for three seconds. The IMU suit calibration involved standing in a neutral position (N-Pose) for four seconds, then moving in the space for 15 seconds, and returning to an N-Pose for eight seconds. The N-Pose required participants to remain still in the following position: (1) stand upright on a horizontal surface, (2) have their feet parallel, one foot-width apart, (3) have their back straight, (4) relax their shoulders, (5) have their arms straight alongside their body with their thumbs pointing forwards, and (6) be facing forwards (Xsens Technologies B.V., 2021).

5.3 Data Protocol

The following data collection protocol was a part of a larger project which required participants to perform a series of walking and standing tasks (i.e., seven minutes of treadmill walking, 500 meters of overground indoor walking, 500 meters of outdoor walking, a ~140 m walking loop that included stair ascend/descend portions, four ~6 m walking trials over force

plates, two quiet standing trials) while wearing the instrumented insoles and IMU suit. However, solely the treadmill data was analyzed for the present thesis. Prior to starting the data collection, the participants were asked to walk on the treadmill to find their preferred walking speed (PWS), while blinded to the speed of the treadmill. The PWS was defined as the speed normally used during daily living activities (Menéndez et al., 2019), and was determined based on the protocol of Dingwell and Marin (2006). Specifically, to find the participant's PWS, they were asked to start walking on the treadmill at their self-identified PWS after which the speed was increased by increments of 0.1 miles per hour by the experimenter until the participant verbally expressed that they were walking at a speed that is "faster than preferred." The value was recorded, and the speed was decreased by increments of 0.1 miles per hour until the "slower than preferred" speed was found. The protocol was repeated two more times, for a total of three times. The average of the three faster-than-preferred and the three slower-than-preferred speeds was taken as their PWS (Dingwell & Marin, 2006). The participants then performed the seven-minute walking trial at their PWS while their movements and plantar pressures were being recorded by the IMU motion capture suit at 240 Hz and the instrumented insoles at 100 Hz. The participants were given the opportunity to take a break prior to the start of the trial to mitigate the possible effects of fatigue accumulated throughout the larger protocol on their gait patterns.

5.4 Data Processing

Following data collection, the pressure, accelerometer, and gyroscope data were exported from the instrumented insoles via the smartphone application into a comma separated (.csv) file. The kinematic data from the IMU suit were retrieved from the computer and processed using the high-definition reprocessing tool in the Xsens software (MVN Analyze 2021, Xsens, Netherlands). The high-definition kinematic data were then exported into a proprietary file format (.mvnx). Position was calculated for the instrumented insoles based on orientation estimation through

Madgwick and colleagues' (2011) sensor fusion algorithm. Using the preprocessed data from the IMU suit and the instrumented insoles, gait events were identified, from which 200 strides were extracted for stability and variability computations.

5.4.1 Gait Detection

Gait cycles were identified from the data collected with the IMU suit using the proprietary algorithms provided in the Xsens software development kit in Matlab (R2022a, Mathworks, United States). The proprietary algorithms identified foot contacts, which act as gait events, from the kinematic data of the foot. The linear acceleration and angular velocities were extracted for both feet segments and the T8 segment, which is representative of the trunk motion.

The data from the instrumented insoles were separated into gait cycles using a custom gait detection algorithm developed in the Python programming language (3.10.2, Python Software Foundation, United States). The gait detection algorithm is reliant on the pressure data (Equation 5.1) to identify the frames during which the foot is in contact with the floor (Chatzaki et al., 2021).

$$Pressure\ Threshold = \min + (\max - \min) \times Pressure\ Factor \quad (Eq. 5.1)$$

If the pressure data exceeded the pressure threshold, then the foot was considered in contact with the floor, with the first frame over the threshold being the heel strike moment and the last frame being the toe off moment. In Equation 5.1, “min” represents the minimum pressure recorded during a stride and the “max” the maximum pressure recorded. The “Pressure Factor” was set at 0.07 for the heel and toe pressure sensors and 0.05 for the midfoot pressure sensors following the methodology from Chatzaki and colleagues (2021). The heel pressure sensor was located underneath the calcaneus, the midfoot pressure sensor was located underneath the medial arch of the foot, and the forefoot pressure was captured by the sum of three pressure sensors located beneath the metatarsophalangeal joints (Appendix C). The most anterior pressure sensor, located

underneath the first and second toes, was not used as it did not reliably record plantar pressure across participants.

The data from the IMU suit and the instrumented insoles were time-synchronized using the toe-off event from corresponding strides. The data for 200 continuous strides were extracted to allow for optimal statistical precision following the recommendations of Bruijn and colleagues (2009a) and Owings and Grabiner (2003). To ensure that the extracted data were representative of steady-state walking, the 200 strides were extracted from 140 seconds onwards. The delay removes the time required for the treadmill to reach the participant's PWS (~20 seconds) and removes 120 seconds of walking at that PWS to ensure the analyzed data is extracted from steady-state walking.

5.4.2 Calculating Variability

Gait variability was calculated from the instrumented insole data following two methods: 1) through gait spatiotemporal analysis (i.e., Stride time, Stance time, Swing time, Double support time, Single support time, Step time, Cadence, Stride length, and Stride velocity), and 2) through kinematic signal analysis (x , y , z components of the acceleration and the pitch, roll, yaw components of the angular velocity as well as the Euclidean norm of each signal for both left and right feet). The mean, standard deviation, and coefficient of variation (CoV), which was calculated as the ratio of the standard deviation to the mean, were calculated for each parameter as the CoV is the most prevalent variability metric found in the literature (König et al., 2016; Kroneberg et al., 2019; Moon et al., 2016). Following the recommendations of Chau and colleagues (2005), the median absolute deviation (MAD; Equation 5.2), which is found to be the most robust variability summary metric, was also calculated to characterize gait variability

$$\text{Median Absolute Deviation} = \text{median}(|x_i - \tilde{x}|) \quad (\text{Eq. 5.2})$$

where x_i represents each value and \tilde{x} is the median value of the dataset. In total, 128 gait variability measures were calculated for the instrumented insoles. Of those, 60 measures represented unilateral variability (15 parameters (7 spatiotemporal (e.g., stride time) and 8 kinematic (e.g., mean yaw variability)) x 4 variability metrics), and eight measures represented bilateral (2 parameters (i.e., step time and cadence) x 4 variability metrics). The unilateral variability measures were initially calculated separately for the left and right feet, and then averaged together. Consequently, each participant had 68 summary variability measures, 36 spatiotemporal and 32 kinematic.

5.4.2.1 Spatiotemporal Variability

Spatiotemporal parameters were calculated using custom Matlab codes (Figure 5.1). The temporal parameters (i.e., Stride time, Stance time, Swing time, Double support time, Single support time, Step time, and Cadence) were calculated based on elapsed time between gait events following the equations used by Chatzaki and colleagues (2021; Equations 5.3 - 5.10)

$$\text{Stride Time (s)} = \text{Heel Strike}_{i+1} - \text{Heel Strike}_i \quad (\text{Eq. 5.3})$$

$$\text{Stance Time (s)} = \text{Toe Off}_i - \text{Heel Strike}_i \quad (\text{Eq. 5.4})$$

$$\text{Single Support Time (s)} = \text{Heel Strike}_j - \text{Toe Off}_j \quad (\text{Eq. 5.5})$$

$$\text{Double Support Time (s)} = (\text{Toe Off}_j - \text{Heel Strike}_i) + (\text{Toe Off}_i - \text{Heel Strike}_{j+1}) \quad (\text{Eq. 5.6})$$

$$\text{Step Time (s)} = \text{Heel Strike}_j - \text{Heel Strike}_i \quad (\text{Eq. 5.7})$$

$$\text{Cadence} \left(\frac{\text{Steps}}{\text{min}} \right) = \frac{60}{\text{Step Time}} \quad (\text{Eq. 5.8})$$

where i is a stride on the side of interest and j is a stride on the contralateral side. Swing time was computed as the single support time of the contralateral foot.

Foot position in 3D was obtained using Madgwick's complementary filter for sensor fusion using the instrumented insole's gyroscope and accelerometer data (Madgwick et al., 2011). From the insole's 3D positions, spatial parameters (i.e., Stride length, Stride velocity) were calculated. Stride length was measured following the distance between two points in 3-dimensional space formula (Equation 5.9)

$$\textit{Stride Length (m)} = \sqrt{(x_2 - x_1)^2 + (y_2 - y_1)^2 + (z_2 - z_1)^2} \quad (\text{Eq. 5.9})$$

where x represents position in the mediolateral direction, y represents position in the anteroposterior direction, and z represents position in the vertical direction. Subscript 1 represents the insole position at heel strike, and subscript 2 represents the insole position at the subsequent heel strike. Stride velocity was calculated following the equation of Chatzaki and colleagues (2021; Equation 5.10)

$$\textit{Stride Velocity} \left(\frac{m}{s} \right) = \frac{\textit{Stride Length}}{\textit{Stride Time}} \quad (\text{Eq. 5.10})$$

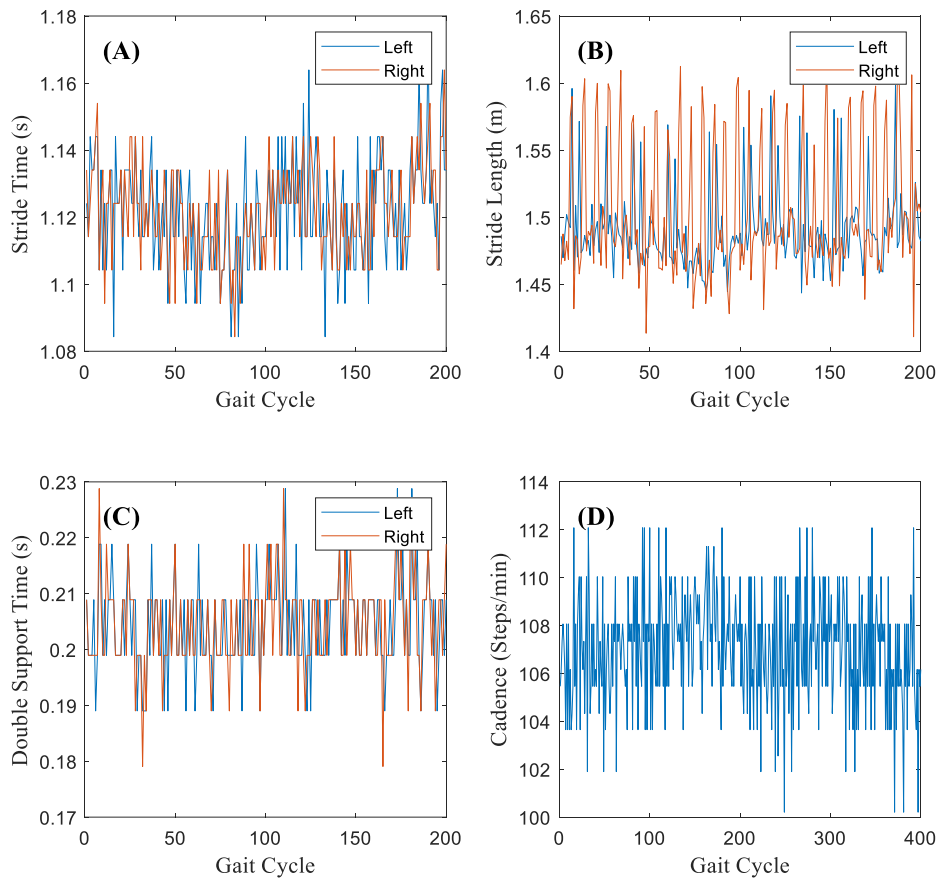


Figure 5.1 Stride-to-stride spatiotemporal parameters calculated from the instrumented insoles for 200 consecutive strides. (A) Stride time (s) for the right foot; (B) Stride length (m) for the right foot; (C) Double-support time (s) for the right foot; (D) Cadence (steps/min).

Unilateral spatiotemporal parameters (e.g., stride time, stride length, double support time) were initially calculated for each foot separately. The final spatiotemporal variability metrics were taken as the average of the right and left foot values. Therefore, 36 spatiotemporal variability measures were included in the final analysis, per participant.

5.4.2.2 Kinematic Variability

The calculations for stride-to-stride kinematic variability measures were based on the methodology from (Toebes et al., 2012). The six time-series (i.e., x , y , z acceleration and pitch, roll, yaw angular velocity) for each foot were time-normalized (0-100%) for each of the 200

strides. Further, the Euclidean norm, or magnitude of a signal, was taken for each sensor (Equation 5.11)

$$\|x\|_2 = \sqrt{\sum_{k=1}^n |x_k|^2} \quad (\text{Eq. 5.11})$$

where x is a vector of dimension n with coordinates x_k .

The MAD was calculated at each 1% increment of the time-normalized gait cycles for the six time-series and the Euclidian norm of both the accelerometer and gyroscope data (Figure 5.2). The summary variability metrics (i.e., mean, SD, CoV, and MAD) were calculated for each signal from the MAD values of each 1% increment of the gait cycle at each foot. The final kinematic variability measures were taken as the average of the right and left foot values. Therefore, 32 kinematic variability measures were included in the final analysis, per participant.

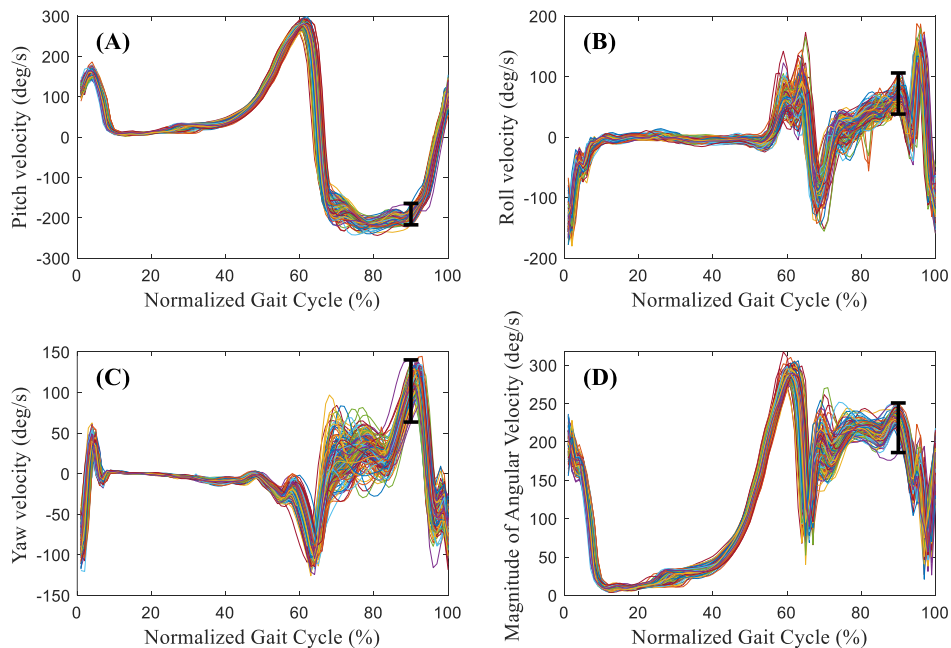


Figure 5.2 Overlay of the angular velocity output for 200 consecutive normalized right-foot strides with black bars illustrating stride-to-stride dispersion at 90% of the gait cycle. (A) Pitch velocity (deg/s); (B) Roll velocity (deg/s); (C) Yaw velocity (deg/s); (D) Euclidian norm of angular velocity (deg/s).

5.4.3 Calculating Local Dynamic Stability

Local dynamic stability was calculated at the trunk and at the feet with the data from the IMU motion capture suit and at the foot only with the data from the instrumented insoles. The data from each system and segment were analyzed individually to estimate LDS: five computations were performed per participant (i.e., three from the IMU suit and two from the insoles). The data from the 200 synchronized continuous strides extracted from each system were normalized to 20,000 points to have an average 100 points per stride. A 12-dimensional state space (Equation 5.12) was reconstructed using the normalized gyroscope and accelerometer data as state variables (Kang & Dingwell, 2009). The state variables were composed of the angular velocities ($\dot{\theta}, \dot{\phi}, \dot{\psi}$) and linear accelerations ($\ddot{x}, \ddot{y}, \ddot{z}$) and their time-delayed copies. A time-delay (τ) of 10 frames with 2 embedding dimensions was used based on the first minimum in the average mutual information function (Fraser & Swinney, 1986), and the false-nearest neighbours function (Kennel et al., 1992), respectively.

$$S(t) = [\ddot{x}(t), \ddot{y}(t), \ddot{z}(t), \dot{\theta}(t), \dot{\phi}(t), \dot{\psi}(t), \ddot{x}(t + \tau), \ddot{y}(t + \tau), \ddot{z}(t + \tau), \dot{\theta}(t + \tau), \dot{\phi}(t + \tau), \dot{\psi}(t + \tau)] \quad (\text{Eq. 5.12})$$

From the constructed state space, LDS was computed using the built-in lyapunovExponent function from the predictive maintenance toolbox in Matlab. The short-term maximum finite-time Lyapunov exponent was calculated over 0 - 0.5 strides for each foot independently for both the instrumented insoles and the IMU suit, as well as for the trunk for the IMU suit. Final foot LDS was taken as the average of the right and left foot for both the instrumented insoles and the IMU suit. Therefore, three LDS measures were included in the final analysis (i.e., foot LDS from instrumented insoles, foot LDS from IMU suit, trunk LDS from IMU suit).

5.5 Statistical Analysis

Three statistical analyses were conducted: 1) intraclass correlation coefficients, 2) simple linear regression, 3) multiple linear regression. To perform the analyses, the dataset consisted of 71 values per participant (i.e., 68 variability values and 3 LDS values).

The foot LDS measured with the instrumented insoles was compared to the values measured using the IMU suit through intraclass correlation coefficients (ICC) to assess the reliability of the instrumented insole results. The LDS values computed at the feet for both systems were then compared to those computed at the trunk using the IMU suit. A two-way mixed effect, consistency, single rater ($ICC_{3,1}$; Equation 5.14) ICC form was chosen for this analysis. A two-way mixed effects model was chosen as the raters (i.e., the instrumented insoles and the IMU suit) are the only raters of interest to this analysis. An ICC form assessing consistency between raters was selected for this analysis as the LDS results for both systems are expected to have a systematic error caused by sensor placement

$$ICC_{3,1} = \frac{MS_R - MS_E}{MS_R + (k - 1)MS_E} \quad (\text{Eq. 5.13})$$

where MS_R = Mean Square for rows; MS_E = Mean Square for error; and k = number of raters/measurements.

ICC values < 0.5 were interpreted as poor reliability, values between 0.5 and 0.75 were interpreted as moderate reliability, values between 0.75 and 0.9 were interpreted as good reliability, and values greater than 0.9 were interpreted as excellent reliability (Cohen, 1988; Koo & Li, 2016).

Two linear regression analyses were performed to estimate trunk LDS. First, a simple linear regression (SLR) analysis was used to predict trunk LDS using the λ_{\max} values calculated at the

feet using the instrumented insole data. The SLR model provided a baseline for trunk LDS prediction using a single predictor variable. The complexity of the prediction model was then increased by using a multiple linear regression (MLR) consisting of five predictor variables. A model containing five predictor variables surpasses the minimal requirement of two subjects per variable (Austin & Steyerberg, 2015), while including variables that quantify several aspects of the gait pattern.

The subset of predictor variables to include in the MLR analysis was selected following an exhaustive approach, where every combination of five predictor variables was selected from the set of 69 possible variables measured for each foot (i.e., 68 variability metrics, 1 stability metric; Appendix E). The exhaustive trial and error combination testing was completed using a custom Matlab script. The predictor variable combination that yielded the highest adjusted R^2 value was retained. All linear regression assumptions (i.e., the independence of observation, linear relationship, homoscedasticity of residuals, multicollinearity, and the normal distribution assumption) were assessed for the retained model. Further, the presence of outliers, influential points, and/or leverage points was assessed. Outliers were defined as subjects with standardized residuals greater than ± 3 standard deviations. Leverage points were considered safe ≤ 0.2 ; $0.2 <$ leverage point ≤ 0.5 were considered risky, and values > 0.5 were considered dangerous (Huber, 1981). Influential points were assessed with Cook's distance values, where values > 1 should be investigated.

The overall model fit was assessed through the adjusted R^2 value. The adjusted R^2 value was used as it is found to incur minimal bias relative to the conventional R^2 with low subject to variable ratios (Austin & Steyerberg, 2015). Nonetheless, both the adjusted and conventional R^2 values are reported to demonstrate the difference in variance explained caused by the bias

correction of the adjusted R^2 . The statistical significance of each regression model was determined using a regression ANOVA with an alpha level of $p < 0.05$. The final regression equations to predict trunk stability using data from the instrumented insoles was produced from the unstandardized coefficients that significantly contributed to the accuracy of the model. The inclusion of predictor variables was determined using a t-test with an alpha level of $p < 0.05$. All statistical analyses were completed in SPSS Statistics (Version 27, IBM, USA). The accuracy of the prediction models (i.e., simple and multiple) was evaluated using the mean percentage of error (Equation 5.14) between predicted and true trunk λ_{max} values, as well as through root mean square error (RMSE; Equation 5.15).

$$Mean\ Error\ (\%) = \frac{Predicted\ \lambda_{max} - True\ \lambda_{max}}{True\ \lambda_{max}} \times 100 \quad (Eq. 5.14)$$

$$RMSE = \sqrt{\sum_{i=1}^n \frac{(Predicted\ \lambda_{max_i} - True\ \lambda_{max_i})^2}{n}} \quad (Eq. 5.15)$$

Chapter 6: Results

6.1 Metric Calculation

In total, 71 metrics were calculated for each participant (Table 6.1). Stride-to-stride variability metrics consisted of nine spatiotemporal parameters and eight kinematic parameters from which the mean, standard deviation, median absolute deviation, and coefficient of variation were calculated. The mean λ_{\max} measured at the foot with the instrumented insoles was greater than that measured with the IMU suit by 0.255, and than the trunk λ_{\max} by 0.798. The mean λ_{\max} measured with the IMU suit at the foot was greater than that measured at the trunk by 0.543.

Table 6.1 Mean of instrumented insole derived variability and stability metrics as well as inertial measurement unit suit derived foot and trunk stability metrics with standard deviations across 200 strides.

Parameter	Mean (SD)	SD (SD)	MAD (SD)	CoV (SD)
Stride Time (s)	1.133 (0.083)	0.014 (0.005)	0.010 (0.003)	0.013 (0.004)
Stance Time (s)	0.666 (0.062)	0.010 (0.003)	0.008 (0.004)	0.016 (0.004)
Swing Time (s)	0.467 (0.026)	0.010 (0.003)	0.008 (0.004)	0.021 (0.006)
Double Support Time (s)	0.199 (0.044)	0.009 (0.002)	0.007 (0.004)	0.044 (0.008)
Single Support Time (s)	0.467 (0.026)	0.010 (0.003)	0.008 (0.004)	0.021 (0.006)
Stride Length (m)	1.429 (0.144)	0.043 (0.010)	0.020 (0.008)	0.030 (0.007)
Stride Velocity (m/s)	1.274 (0.187)	0.038 (0.010)	0.016 (0.006)	0.030 (0.006)
Step Time (s)	0.566 (0.042)	0.024 (0.016)	0.022 (0.017)	0.042 (0.028)
Cadence (Steps/min)	106.7 (7.255)	4.410 (2.923)	3.950 (2.919)	0.042 (0.028)
ML Acc (m/s ²)	0.740 (0.144)	0.769 (0.237)	0.350 (0.103)	1.028 (0.184)
AP Acc (m/s ²)	0.944 (0.141)	1.573 (0.306)	0.336 (0.082)	1.666 (0.208)
V Acc (m/s ²)	0.801 (0.150)	0.895 (0.227)	0.409 (0.100)	1.111 (0.136)
Magnitude of Acceleration (m/s ²)	0.890 (0.153)	1.209 (0.299)	0.414 (0.091)	1.353 (0.194)
Pitch (degs/s)	7.350 (1.003)	6.667 (2.010)	3.796 (0.793)	1.122 (0.090)
Roll (degs/s)	6.644 (1.448)	5.649 (1.626)	3.467 (1.301)	0.844 (0.121)
Yaw (degs/s)	5.149 (1.115)	4.973 (1.049)	3.086 (0.854)	0.968 (0.053)
Magnitude of Angular Velocity (degs/s)	6.946 (0.979)	6.373 (1.166)	3.675 (0.846)	0.917 (0.107)

Foot Stability (Insoles)	1.519 (0.117)	-	-	-
Foot Stability (IMU)	1.264 (0.128)	-	-	-
Trunk Stability (IMU)	0.721 (0.116)	-	-	-

Abbreviations: SD, Standard Deviation; MAD, Median Absolute Deviation; CoV, Coefficient of Variation; ML: Mediolateral; AP; Anteroposterior; V: Vertical; Acc: Acceleration.

6.2 Local Dynamic Stability Correlations

Intraclass correlation coefficient estimates, and their 95% confidence intervals, were calculated using a two-way mixed effect, consistency, single rater model (ICC_{3,1}) to assess the inter-rater reliability of the LDS estimates (Table 6.2). The ICC between the estimates of trunk stability obtained from the IMU suit and those obtained from the instrumented insoles revealed a moderate inter-rater reliability. Similarly, the ICC between the trunk stability estimates and the foot stability estimates, both measured using the IMU suit, revealed a moderate inter-rater reliability. The foot LDS estimate measured using the instrumented insoles and the IMU suit revealed a good inter-rater reliability. All analyses yielded statistically significant results ($p < 0.05$), indicating that the inter-rater reliability estimates are significantly different from zero.

Table 6.2 Intraclass correlation coefficients for local dynamic stability values between measurement tools and body segments.

Raters	ICC _{3,1} [95% CI]	Value	d.f. ²	Sig.
Trunk LDS vs. Insoles LDS	0.641 [0.211, 0.863]	4.576	14	0.004
Trunk LDS vs. IMU LDS	0.625 [0.313, 0.923]	4.338	14	0.005
Insole LDS vs. IMU LDS	0.860 [0.775, 0.975]	13.26	14	<0.001

Note: Intraclass correlation coefficient with a two-way mixed effect, consistency, single rater model (ICC_{3,1}). Trunk LDS is measured with the IMU suit. Insole LDS is foot stability measured with the instrumented insoles. IMU LDS is foot stability measured with the IMU suit.

Abbreviations: ICC: Intraclass correlation coefficient; 95% CI: 95% confidence interval; d.f.: degrees of freedom; Sig.: Significance; IMU: Inertial measurement unit; LDS: Local dynamic stability.

The SLR model using foot stability as a predictor for trunk stability statistically significantly predicted trunk LDS, $F(1, 13) = 9.148$, $p < 0.010$, $R^2 = 0.413$, adj. $R^2 = 0.368$. The

trunk stability estimates had a mean error of 9.861% and a root mean square error (RMSE) of 0.087 (Figure 6.4).

6.3 Multiple Linear Regression

A subset of five predictor variables was selected from the set of 69 potential variability and stability measures. The exhaustive predictor variable combination testing identified the regression model composed of the *stride time standard deviation*, *double support time standard deviation*, *single support time mean*, *mean yaw variability*, and *median absolute deviation of yaw variability* as the combination that explained the most variance in predicting trunk stability (Table 6.3).

Prior to building an MLR model from those variables, the six assumptions (i.e., independence of observations, linearity, homoscedasticity of residuals, multicollinearity, normal distribution, and no significant outliers or leverage/influential points) were tested to ascertain the fit of the data to the ANOVA for regression model. The independence of observations assumption was statistically tested using the Durbin-Watson test. The result of the Durbin-Watson value was 1.654, which is within the accepted range of [1.5, 2.5] to demonstrate independence of residuals; no correlation between residuals exists. The linear relationship between the dependent variable and the independent variables was assessed using the unstandardized predicted value and studentized residuals plot (Figure 6.1), as well as all partial plots produce in SPSS. From Figure 6.1, the assumption of homoscedasticity is confirmed as the residuals appear randomly scattered. The multicollinearity assumption was met as all VIF values are below 10 (Table 6.3).

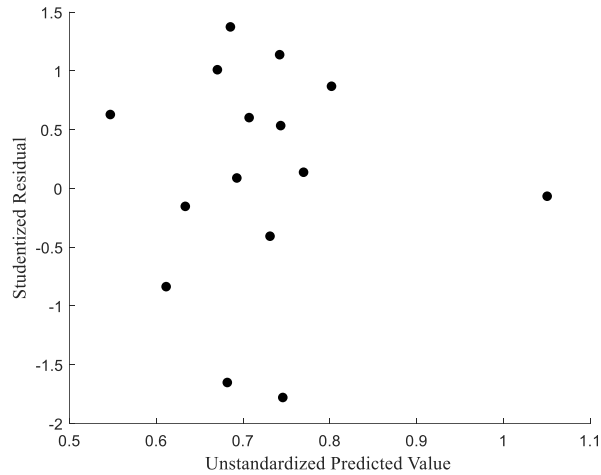


Figure 6.1 Unstandardized predicted values and studentized residuals.

Note: No correlation exists between the studentized residuals and the unstandardized predicted values.

From the data of the 15 participants, no outliers were identified. Further, no highly influential points were detected in the sample based on Cook’s distance values (Figure 6.2). However, three dangerous leverage points were detected in the sample (Figure 6.2). Upon inspection of the data, the values from the participants exhibiting dangerous leverage were deemed valid and, therefore, were retained in the analysis.

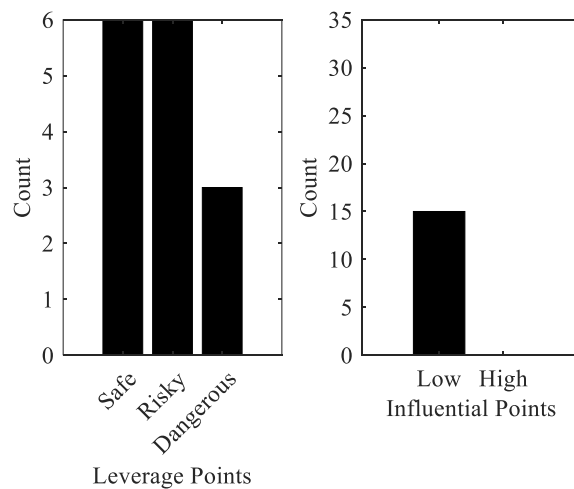


Figure 6.2 Leverage and influential points.

Note: (A) Leverage points in the sample size ($0 \leq \text{Safe} < 0.2$; $0.2 \leq \text{Risky} < 0.5$; $0.5 \leq \text{Dangerous}$). (B) Highly influential points ($0 \leq \text{Low} < 1$; $1 \leq \text{High}$).

The normality assumption was assessed using a quantile-quantile (Q-Q) plot (Figure 6.3). Further, the probability-probability (P-P) plot and the histogram with superimposed normal curve generated by SPSS were inspected to ascertain the normal distribution of the residuals.

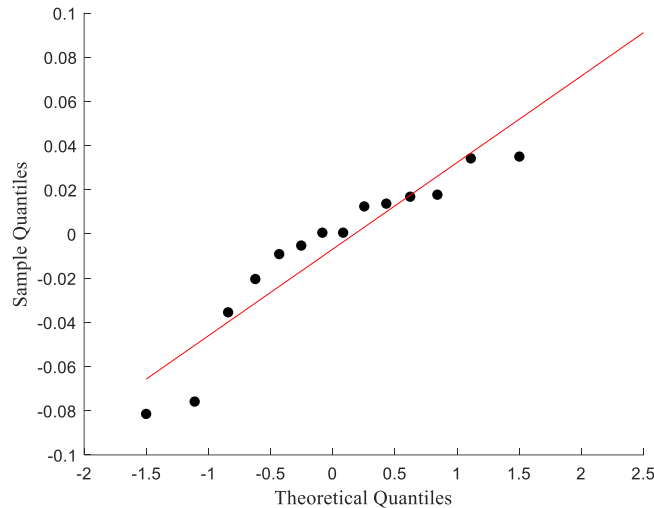


Figure 6.3 Normal Q-Q plot of standardized residuals.

Since all MLR assumptions were met, the MLR model was implemented. The coefficients of the model, as well as the t-values results for each predictor variable, are shown in Table 6.3. The MLR model statistically significantly predicted trunk local dynamic stability, $F(5, 9) = 16.267$, $p < 0.001$, $R^2 = 0.900$, $\text{adj. } R^2 = 0.845$. The MLR model explained 47.7% more variance than the SLR model. Stride time standard deviation, double support time standard deviation, mean yaw variability, and the MAD of yaw variability added significantly to the trunk local dynamic stability prediction, $p < 0.05$ (Table 6.3). Mean single support time and the constant term did not add significantly to the trunk local dynamic stability prediction (Table 6.3). Equation 6.1 uses the unstandardized coefficients (Table 6.3) to estimate trunk LDS using variability metrics derived from the instrumented insoles data. The trunk stability predictions had a mean error of 3.99% and an RMSE of 0.036 with the constant and mean single support time added to the model. A reduced MLR model containing stride time standard deviation, double support time standard deviation,

mean yaw variability, and the MAD of yaw variability as predictors was also obtained. The reduced MLR model also statistically significantly predicted trunk local dynamic stability, $F(4, 10) = 18.677, p < 0.001, R^2 = 0.882, \text{adj. } R^2 = 0.835$. The reduced MLR model explained 46.7% more variance than the SLR model, and 1.0% less variance than the full MLR model. Using the reduced MLR model, trunk stability predictions had a mean error of 4.82% and an RMSE of 0.039 (Figure 6.4).

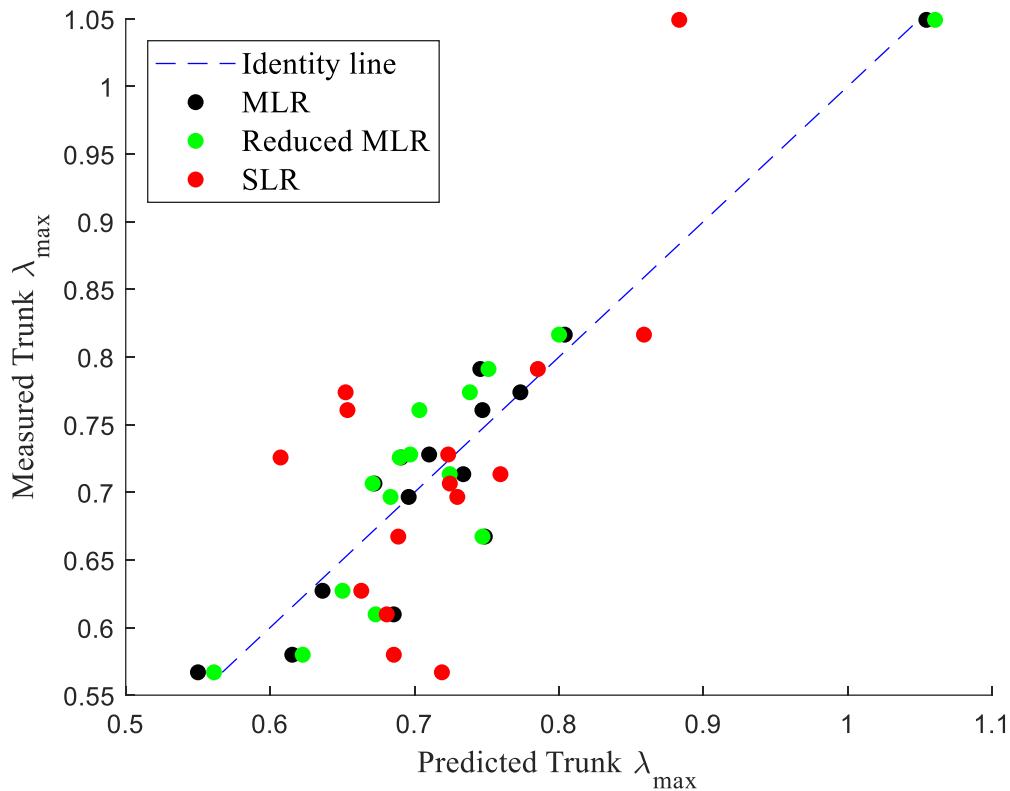


Figure 6.4 Regression models fit for trunk local dynamic stability prediction.

Note: the multiple linear regression (MLR) model to predict trunk local dynamic stability (LDS) from 5 predictor variables (black), the MLR with mean single support time removed (green) and the simple linear regression (SLR) from foot LDS (red) are represented with the identity line (blue).

Note: The isolated trunk λ_{\max} values represent the trunk stability of the participant in the 55-60 years of age group.

Table 6.3 Model summary with correlations and collinearity statistics.

Model	Unstandardized Coefficient		Standardized coefficient Beta	t-test (<i>p</i> -value)	Correlations			Collinearity Statistics	
	β [95% CI]	Std. error			Zero-order	Partial	Part	Tolerance	VIF
ST SD	26.95 [12.65, 41.26]	6.323	1.163	4.262 (0.002)	0.709	0.818	0.448	0.149	6.730
DST SD	-59.45 [-87.80, -31.11]	12.53	-1.071	-4.745 (0.001)	0.321	-0.845	-0.499	0.217	4.598
SST Mean	1.165 [-0.878, 3.208]	0.903	0.250	1.290 (0.229)	0.511	0.395	0.136	0.294	3.400
Mean Yaw Var	0.070 [0.016, 0.123]	0.024	0.652	2.944 (0.016)	0.315	0.700	0.310	0.226	4.430
MAD Yaw Var	-0.101 [-0.172, -0.031]	0.031	-0.710	-3.246 (0.010)	-0.121	-0.734	-0.342	0.232	4.318
Constant	0.253 [-0.746, 1.253]	0.442	-	0.573 (0.581)	-	-	-	-	-

Note: Statistical significance, $p < 0.05$.

Abbreviations: SD: Standard deviation; ST: Stride time; DST: Double support time; SST: Single support time; Var: Variability; MAD: Median absolute deviation.

$$Trunk \lambda_{max} = 26.95 \times ST \ SD - 59.45 \times DST \ SD + 1.165 \times \overline{SST} + 0.070 \times \overline{\psi \ var} - 0.101 \times MAD \ \psi \ var + 0.253 \quad (\text{Eq. 6.1})$$

Where ST SD represents the stride time standard deviation, DST SD represents the double support time standard deviation, \overline{SST} represents single support time mean, $\overline{\psi \ var}$ represents the mean of ψ variability, and MAD ψ var represents the median absolute deviation of ψ variability.

Chapter 7: Discussion

Real-world gait stability assessments can help in the identification of individuals at increased fall risk. To date, gait stability assessments are primarily conducted by measuring trunk kinematics, as the trunk segment was successfully used to discriminate between fallers and non-fallers (Toebe et al., 2012). The trunk segment is also found to be a more sensitive marker of gait impairments than lower body segments (Kang & Dingwell, 2009). However, real-world trunk stability assessments are impractical and prone to errors caused by sensor placement. Therefore, the aim of this work was to build an MLR model to estimate trunk LDS from data collected using instrumented insoles during steady-state walking on a treadmill at a preferred speed. The accelerometer, gyroscope, and pressure sensors embedded in the instrumented insoles provided the data necessary to: 1) identify gait events to extract 200 strides for analysis, 2) calculate foot and trunk LDS, 3) calculate spatiotemporal and kinematic variability, and 4) estimate trunk LDS through an MLR model. It was hypothesized that there would be good reliability between foot LDS values measured from the instrumented insoles data and the IMU suit data. It was also hypothesized that the best trunk LDS estimations would be found using a combination of foot LDS values, spatiotemporal variability, and kinematic variability. The results show that foot LDS values measured with the instrumented insoles are reliable to use when compared to the IMU suit, which was previously validated for gait kinematics (Zhang et al., 2013). However, foot LDS explains little variance in trunk LDS values. A combination of spatiotemporal and kinematic variability metrics (i.e., stride time standard deviation, double support time standard deviation, single support time mean, mean yaw variability, and median absolute deviation of yaw variability) was found to best predict trunk LDS.

The ICC results between the foot LDS estimates measured through the instrumented insoles and the IMU suit suggest high levels of agreement and consistency between systems (ICC_{3,1} of 0.860), indicating that the instrumented insoles adequately capture foot stability. Although a mean offset in foot local dynamic stability was found between the two systems (0.255), the ICC results support the hypothesis

that foot LDS can be reliably calculated with the instrumented insoles. The offset found between the two systems can be due to the placement of the IMU sensor (i.e., instrumented insoles: under the medial arch of the foot; IMU suit: above the cuneiform bones), which caused differences in the orientation of the sensors. Differences in sensor orientation are a concern previously raised by van Schooten and colleagues (2013) for inter-session repeatability and reliability of trunk LDS measurements as they found poor reliability between sessions. Although no studies to date have compared λ_{\max} values between IMUs for the same segment, it is evident that sensor placement affects the outcome measures of stability. While the effect of IMU characteristics (e.g., bias, sample rate, resolution, range, noise, etc.) on LDS values is unknown, it is possible that differences between the IMU sensors embedded in the instrumented insoles and those of the Xsens MVN suit exist, which could also have affected the λ_{\max} values calculated between systems.

The larger LDS values found at the feet relative to the trunk indicate that the foot is more locally unstable than the trunk. The LDS differences between segments is consistent with the results of Kang and Dingwell (2009) who attribute the findings to the greater inertia of the trunk, which aids in perturbation attenuation. Further, they found a gradual increase in LDS from distal segments to proximal segments (Kang & Dingwell, 2009), which is indicative of the continuous attenuation of perturbations along the kinematic chain. The moderate inter-rater reliability between the feet and the trunk LDS estimates ($ICC_{3,1}$ of 0.641 and 0.625 for foot stability measured by the insoles and the IMU suit respectively) suggests a moderate level of consistency and agreement between foot stability and trunk stability. Therefore, measuring LDS at the level of the feet does not appropriately represent the stability of the trunk and, by extension, whole-body stability as the trunk is deemed the base of all functional movements (Karthikbabu et al., 2011).

The SLR model using foot LDS from the instrumented insoles to predict trunk LDS explained a low amount of the total variance in the data. The SLR model reflects the simplest prediction model, whereby trunk LDS is solely explained by foot LDS. The low fit of the SLR model supports the moderate reliability values found between LDS values at the foot and at the trunk. The low fit of the model to the data reflects the complex relationship that exists between the trunk and the feet. During gait, the locomotor system is subject to perturbations that can arise from both internal and external sources. By using a controlled environment in the present study (i.e., walking on a treadmill), the perturbations experienced are limited to the internal factors that cause deviations from the normal state of the system; external sources such as uneven surfaces are removed. The exception being the feet. Throughout gait, the feet are subject to external perturbations as foot placement can vary from stride-to-stride and cause variation in the ground reaction forces received by the feet. The variation in foot placement may be due to unplanned internal perturbations that alter lower limb kinematics. Based on Kang and Dingwell's (2009) findings, it can be hypothesized that the external perturbations encountered at the foot are then attenuated along the kinematic chain, and minimized before reaching the trunk. Conversely, the trunk is influenced by the movements of the lower limbs and the upper limbs, which play a stabilizing role during gait (Ortega et al., 2008) and aid in the recovery from perturbations (Bruijn, Meijer, et al., 2010). Meaning that, while the feet experience the influence of both internal and external perturbations, the trunk segment receives the minimized effects of the external perturbations from the lower limbs, and its stability is improved by the movements of the upper limbs. The moderate reliability found between the feet and trunk LDS, as well as the low model fit of the SLR model, supports the need to supplement foot LDS with other metrics to best predict trunk LDS. Through an MLR, which reflects multiple aspects of an individual's gait pattern, the accuracy of trunk LDS predictions can be improved.

The main objective of this study was to find the combination of stability and variability metrics to predict trunk LDS. The MLR model that explains the greatest amount of variance in trunk LDS from five predictor variables reached an adjusted R^2 value of 0.845, an increase of 0.477 relative to the SLR. The model was composed of spatiotemporal and kinematic variability metrics, without the addition of foot stability. The identified predictor variable combination refutes the original hypothesis as it was expected that a combination of foot stability and variability metrics would best predict trunk LDS. Specifically, it appears that temporal variability parameters and angular velocity variability are the most relevant in the prediction of trunk stability. However, mean single support time was found to be non-significant to trunk LDS estimations. A reduced MLR containing stride time standard deviation, double support time standard deviation, mean yaw variability, and the MAD of yaw variability reached an adjusted R^2 value of 0.835, an increase of 0.467 relative to the SLR, and a decrease of 0.01 relative to the full MLR. Moreover, the constant term in the full MLR model is found to be statistically insignificant, indicating that the trunk LDS value is not statistically different from zero when the independent variables are all equal to zero. Therefore, in a case of highly rigid gait patterns that exhibit no variability from stride-to-stride, λ_{\max} would be equal to 0, indicating a steady state system where neighbouring trajectories would neither converge ($\lambda_{\max} < 0$) nor diverge ($\lambda_{\max} > 0$).

Stride time can be viewed as the final integrated output from the locomotor system of central and peripheral inputs (Hausdorff et al., 2001). Low stride time variability (STV) represents automaticity in the movement pattern, which results from low motor variations in motor performance from stride-to-stride (Hausdorff, 2007). Therefore, low STV represents a more consistent state that produces more regular outputs, whereas high STV represents lower rhythmicity of the locomotor system. The positive relationship between stride time standard deviation and trunk LDS indicates that more variability in the time between ipsilateral heel strikes leads to more instability. Comparatively, high STV is considered a

good indicator of gait instability in the literature (Beauchet et al., 2007; Hausdorff et al., 2001; Maki, 1997). Increased STV was also previously associated with increased fall risk, decreased physical performance, and decreased functional status (Beauchet et al., 2005, 2009; Dubost et al., 2006; Hausdorff, 2007; Hausdorff et al., 2001). The presence of STV as a predictor for trunk LDS in the current MLR suggests that STV is indeed a good marker of gait instability that could help identify individuals at a high risk of falling.

With regards to DS variability, measured through the standard deviation of DS time, there is a negative relationship with trunk LDS, after adjusting for the other predictor variables. Interestingly, the zero-order correlation between the two variables indicates a positive relationship. Meaning that as DS variability increases, trunk λ_{\max} increases, reflecting decreased stability. However, when controlling for the influence of the other predictor variables, as DS variability increases, trunk λ_{\max} decreases, reflecting increased stability. The reversal in the direction of the relationship suggests that in a gait pattern with high STV, high SS time, and high yaw variability, having high DS variability improves trunk stability. The reversal effect observed is evidence of the need for a holistic, multivariate approach to gait stability assessments. By accounting for the influence of other variables on the variable of interest, in this case, DS variability, the true relationship between two variables can be unveiled; failure to do so may lead to inaccurate or misleading interpretations.

During DS, the locomotor system has more control over the movement of the CoM and, consequently, uses this portion of the gait cycle to alter gait and correct deviations (Williams, 2020). Investigations into phase-dependent metabolic costs during gait identified that although step-to-step transitions, which correspond closely with initial DS, accounts for ~20% of the gait cycle, it is where 33% of the net metabolic energy is spent (Umberger, 2010). The high metabolic cost of step-to-step transitions is attributed to the redirection of the center of mass velocity (Umberger, 2010). As part of his doctoral

dissertation, Williams (2020) tasked individuals to walk on a treadmill while altering their gait based on visual feedback to influence the time spent in double support. He found that participants were able to decrease the percentage of time spent in DS but had difficulty increasing the time spent in DS. Based on this finding, Williams (2020) concluded that humans naturally spend the maximal amount of time in DS during locomotion. Given its role in perturbation attenuation, high variability in DS appears to be indicative of continuous adaptations undergone by a healthy locomotor system to the stride-to-stride perturbations it encounters. Specifically, in a highly variable gait pattern, the negative correlation between DS variability and trunk LDS suggests that the locomotor system adjusts the time spent in DS based on the perturbation recovery required. Therefore, continuously adjusting the time spent in DS enables humans to optimize their gait efficiency while remaining stable.

Mean SS time is found to be a non-significant contributor to the full MLR model. However, it is possible that the low sample size available for the present analysis contributed to the lack of significance for mean SS time as a predictor of trunk LDS. As mean SS time was identified as one of the variables that best predicted trunk LDS, it remains important to discuss its importance in gait analysis. In the full MLR model, mean SS time is found to have a positive relationship with trunk LDS. During SS, the center of mass travels outside the base of support, with the greatest separation being at toe off and prior to heel strike (Lugade et al., 2011). During terminal stance, the CoM moves past the forefoot and there is high activation of the gastrocnemius muscles for the anterior propulsion of the body (Lee et al., 2019). Meaning that, while the body is in a controlled forward fall with the CoM is outside the BoS, muscles are activating to generate a forward acceleration of the body. Until the swing leg makes contact with the ground to reestablish a state of equilibrium where the CoM is within the BoS, the individual is in an unstable state (Remelius et al., 2014). Therefore, by increasing the time spent in SS, individuals are increasing the time spent in an unstable state. The inclusion of mean SS in the full MLR model to predict trunk LDS, with a

positive regression coefficient, indicates that individuals who spend more time in SS have a less stable gait pattern.

Yaw (ψ) variability has received little attention in the literature. Yet, the mean ψ variability and the MAD of ψ variability are found to be important predictors for trunk LDS. Interestingly, the two predictors have opposite effects on gait stability, as mean ψ variability is positively correlated to trunk LDS and MAD of ψ variability is negatively correlated. The positive correlation between mean ψ variability and trunk LDS indicates that gait is less stable when the stride-to-stride variability in ψ increases on average. Therefore, a locomotor system that exhibits more stride-to-stride variability across the gait cycle, or one that contains areas of “extreme” variability are associated with decreased stability. As the ψ variability is near zero during the SS phase, a greater mean ψ variability can be indicative of a highly variable DS and/or swing phase. Conversely, the negative correlation between the MAD of ψ variability and trunk LDS indicates that gait is more stable when there is greater dispersion of ψ variability across the gait cycle. From the MAD equation, and the ψ variability present across the gait cycle, it becomes apparent that the MAD of ψ variability will align with the distance between the median ψ variability and the variability in SS (Appendix D). Since the swing and SS phases each account for 40% of the gait cycle (Mirelman et al., 2018), and contain high and low stride-to-stride variability respectively, the main determinant of median ψ variability is the ψ variability observed during DS. Consequently, it can be hypothesized that high ψ variability in DS is indicative of greater adaptability of the locomotor’s correction mechanisms to attenuate the effects of perturbations from stride-to-stride. Specifically, the medial/lateral rotation velocity of the foot during double support will vary from stride-to-stride in response to perturbations in the gait pattern. Therefore, the contrary effects of mean ψ variability and the MAD of ψ variability on trunk LDS suggest that low ψ variability during the swing phase and high ψ variability during DS contribute to a more stable gait pattern.

The MLR model developed in this study uses linear variability metrics to predict a nonlinear measure. The presence of both positive and negative relationships between the predictor variables and trunk LDS is best supported by the optimal movement variability theory. The OMV theory proposes that an optimal amount of variability exists to reflect the adaptability of the underlying system for mature motor skills in healthy individuals. Contrastingly, traditional variability theories (e.g., generalized motor programs theory (Summers & Anson, 2009), uncontrolled manifold hypothesis (Scholz & Schöner, 1999), and dynamic systems theory (Kamm et al., 1990)) suggest that variability decreases as motor performance improves, such that low variability is indicative of a “healthy” locomotor system. The negative correlation between trunk LDS and DS time SD, as well as for the MAD of ψ variability found in this study refute the traditional theories of variability as increased variability does not strictly reflect decreases in motor performance. Rather, the negative correlations provide evidence that increased variability can be indicative of adaptations in the locomotor system, which improve stability. Furthermore, the positive correlations between trunk LDS and ST standard deviation, mean SS time, as well as mean ψ variability suggest that increased variability is indicative of a noisy and unpredictable system, which decreases stability. Further understanding of the adaptations of gait strategies employed by individuals is required to understand the impact variability at each phase of the gait cycle has on gait stability. Specifically, accounting for the effect variability at other phases of the gait cycle has on the variable of interest may reveal underlying stabilizing mechanisms.

Chapter 8: Limitations

The findings of this study present some limitations relating to their generalizability, namely: the population sample, and the controlled walking environment. The population sample consisted primarily of healthy young adults between the ages of 20 and 40, with only one participant between the ages of 55 and 60. While the objective of this work focused on within-subject interactions to predict trunk LDS from instrumented insole-based metrics, the effect of age on stability is apparent in the results. The analysis of a larger age distribution would yield a more generalizable regression equation for the healthy population. Moreover, the findings of this study are limited to a healthy, relatively young, population, and may not apply to a clinical population (e.g., multiple sclerosis, Parkinson's disease, Huntington's, stroke, etc.), who exhibit different gait patterns (Gaßner et al., 2020; Huisinga et al., 2013; Moon et al., 2016; Schmitt et al., 2020; Socie et al., 2013). For this reason, the regression model presented in this study is assumed to be only adequate for healthy adult populations.

The generalizability of these findings is limited to treadmill walking at preferred walking speed. Known differences exist between treadmill walking and overground walking in terms of kinematics and kinetics that demonstrate the two gait patterns are not equivalent (Fukuchi et al., 2018; Murray et al., 1985; Nymark et al., 2005; Riley et al., 2007; Schmitt et al., 2021; Song & Hidler, 2008; Terrier & Dériaz, 2011; Watt et al., 2010; Yang & King, 2016). When comparing treadmill, indoor, and outdoor walking, significant differences in gait velocity, double support percentage, stride length, and cadence were found across conditions (Schmitt et al., 2021). These biomechanical differences may be due to different control strategies employed in the different environments. On the treadmill, the primary goal is not to remain in the same absolute position but rather to maintain the same speed as the treadmill (Dingwell & Cusumano, 2015). However, regulating speed does not appear to be the control strategy employed during overground walking as walking speed is found to vary considerably (Collins & Kuo, 2013).

The small sample size available for the present analysis is another important limitation to the findings of this thesis work. Although surpassing the threshold of two subjects per variable brought forth by Austin and Steyerberg (2015), the small sample size gives rise to large confidence intervals in the findings. Notably, the confidence intervals around the ICC values and the coefficients of the regression equation. It is also suspected that mean SS time is not a statistically significant predictor of trunk LDS due to the small sample size. Moreover, the “dangerous” leverage points may be deemed dangerous because of the small sample size since fewer observations allow any deviation from the sample to be highly influential on the results. Consequently, by increasing the sample size in future work, a more robust regression model can be developed.

From the above evidence, the findings of this study are limited to healthy adult walking on a treadmill at preferred walking speed. Although the predictor variables identified are expected to remain strong predictors in other contexts, it is likely that the weight of the coefficients will require adjustments depending on the environment and population. Further work is necessary to optimize the use of instrumented insoles for trunk LDS estimation in various settings.

Chapter 9: Future work

The findings of this thesis work are a part of a larger overarching project that aims to develop an unobtrusive solution using instrumented insoles to monitor gait changes in people with multiple sclerosis. The methods presented in this thesis provides a base framework for estimating trunk LDS from instrumented insole data. Next steps will involve developing a regression equation that is specific to the gait patterns of people with multiple sclerosis. Moreover, to achieve a truly unobtrusive solution capable of monitoring gait changes from free-living gait data, it will be necessary to implement a method to calculate LDS from multiple short walking bouts.

The current framework will serve as a starting point to develop a regression equation that estimates trunk LDS from instrumented insole data for people with multiple sclerosis. Although it is possible that the regression equation presented in the present work is applicable to the gait patterns of people with multiple sclerosis, it is unlikely given the differences that exist between their gait pattern and that of their healthy counterparts (Chee et al., 2021; Coca-Tapia et al., 2021; Sato et al., 2022). Similarly, it cannot be assumed that the regression equation presented in this work applies to the gait pattern of populations with any neurological disorder. Therefore, further work will be required to develop a regression equation to estimate trunk LDS from instrumented insole data specifically for people with multiple sclerosis.

The current work is limited by the reliance on the treadmill for accurate LDS calculations. Given the final objective of estimating stability in people with multiple sclerosis, it is unfeasible to collect treadmill gait data from individuals with high levels of disability. To overcome this limitation, alternative statistical methods (e.g., bootstrapping) will be required to calculate LDS from multiple short walking bouts (Sloot et al., 2011). By developing a methodology that estimates trunk LDS from multiple short walking bouts with instrumented insoles, gait analysis can be performed in free-living conditions. Consequently, it will be possible to unobtrusively monitor stability in people with multiple sclerosis in real-world settings.

Chapter 10: Conclusion

The MLR model presented in this thesis can predict trunk stability with good accuracy using instrumented insole-derived measures. This study provides further insights into the effects of different aspects of the gait pattern on gait stability. Specifically, increased stride time variability, mean single support time, and mean ψ variability leads to decreased trunk stability, whereas increased double support time variability, and MAD of ψ variability leads to increased trunk stability, when accounting for the other variables. The reversal effect observed with double support time variability highlights the importance of a holistic approach to gait assessments that includes confounding factors in the analysis. Further, it appears that foot stability is only moderately correlated to trunk stability, and that foot stability explains a low amount of variance in trunk stability. The results of this study demonstrate the possible use of instrumented insoles for unobtrusive gait assessments and monitoring. By expanding on this work, instrumented insoles could serve as a screening tool for fall risk in real-life settings across various populations.

Chapter 11: References

- Amboni, M., Barone, P., & Hausdorff, J. M. (2013). Cognitive contributions to gait and falls: Evidence and implications. *Movement Disorders: Official Journal of the Movement Disorder Society*, 28(11), 1520. <https://doi.org/10.1002/MDS.25674>
- Austin, P. C., & Steyerberg, E. W. (2015). The number of subjects per variable required in linear regression analyses. *Journal of Clinical Epidemiology*, 68(6), 627–636. <https://doi.org/10.1016/J.JCLINEPI.2014.12.014>
- Bailey, C. A., Uchida, T. K., Nantel, J., & Graham, R. B. (2021). Validity and sensitivity of an inertial measurement unit-driven biomechanical model of motor variability for gait. *Sensors 2021, Vol. 21, Page 7690, 21(22)*, 7690. <https://doi.org/10.3390/S21227690>
- Beange, K. H. E., Chan, A. D. C., Beaudette, S. M., & Graham, R. B. (2019). Concurrent validity of a wearable IMU for objective assessments of functional movement quality and control of the lumbar spine. *Journal of Biomechanics*, 97, 109356. <https://doi.org/10.1016/j.jbiomech.2019.109356>
- Beauchet, O., Allali, G., Annweiler, C., Bridenbaugh, S., Assal, F., Kressig, R. W., & Herrmann, F. R. (2009). Gait variability among healthy adults: Low and high stride-to-stride variability are both a reflection of gait stability. *Gerontology*, 55(6), 702–706. <https://doi.org/10.1159/000235905>
- Beauchet, O., Allali, G., Berrut, G., & Dubost, V. (2007). Is low lower-limb kinematic variability always an index of stability? *Gait & Posture*, 26(2), 327–328. <https://doi.org/10.1016/J.GAITPOST.2007.02.001>
- Beauchet, O., Dubost, V., Herrmann, F. R., & Kressig, R. W. (2005). Stride-to-stride variability while backward counting among healthy young adults. *Journal of NeuroEngineering and Rehabilitation*, 2(1), 1–8. <https://doi.org/10.1186/1743-0003-2-26/FIGURES/1>
- Berg, W. P., Alessio, H. M., Mills, E. M., & Tong, C. (1997). Circumstances and consequences of falls in independent community-dwelling older adults. *Age and Ageing*, 26(4), 261–268. <https://doi.org/10.1093/AGEING/26.4.261>
- Best, A. N., Martin, J. P., Li, Q., & Wu, A. R. (2019). Stepping behaviour contributes little to balance control against continuous mediolateral trunk perturbations. *Journal of Experimental Biology*, 222(24). <https://doi.org/10.1242/jeb.212787>
- Bisi, M. C., Riva, F., & Stagni, R. (2014). Measures of gait stability: Performance on adults and toddlers at the beginning of independent walking. *Journal of NeuroEngineering and Rehabilitation*, 11(1). <https://doi.org/10.1186/1743-0003-11-131>
- Bizovska, L., Svoboda, Z., Janura, M., Bisi, M. C., & Vuillerme, N. (2018). Local dynamic stability during gait for predicting falls in elderly people: A one-year prospective study. *PLoS ONE*, 13(5). <https://doi.org/10.1371/JOURNAL.PONE.0197091>
- Blair, S. (2019). *Biomechanical Considerations in Goal- Kicking Accuracy: Application of an Inertial Measurement System* [Victoria University]. https://www.researchgate.net/publication/340280090_Biomechanical_Considerations_in_Goal-Kicking_Accuracy_Application_of_an_Inertial_Measurement_System/figures?lo=1#fullTextFileContent
- Blair, S., Duthie, G., Robertson, S., Hopkins, W., & Ball, K. (2018). Concurrent validation of an inertial

measurement system to quantify kicking biomechanics in four football codes. *Journal of Biomechanics*, 73, 24–32. <https://doi.org/10.1016/J.JBIOMECH.2018.03.031>

- Bloch, F., Thibaud, M., Dugué, B., Brèque, C., Rigaud, A.-S., & Kemoun, G. (2010). Episodes of falling among elderly people: A systematic review and meta-analysis of social and demographic predisposing characteristics. *Clinics*, 65(9), 895. <https://doi.org/10.1590/S1807-59322010000900013>
- Bloch, F., Thibaud, M., Tournoux-Facon, C., Brèque, C., Rigaud, A. S., Dugué, B., & Kemoun, G. (2013). Estimation of the risk factors for falls in the elderly: Can meta-analysis provide a valid answer? *Geriatrics & Gerontology International*, 13(2), 250–263. <https://doi.org/10.1111/J.1447-0594.2012.00965.X>
- Brach, J. S., Berlin, J. E., VanSwearingen, J. M., Newman, A. B., & Studenski, S. A. (2005). Too much or too little step width variability is associated with a fall history in older persons who walk at or near normal gait speed. *Journal of Neuroengineering and Rehabilitation*, 2. <https://doi.org/10.1186/1743-0003-2-21>
- Brach, J. S., Studenski, S. A., Perera, S., VanSwearingen, J. M., & Newman, A. B. (2007). Gait variability and the risk of incident mobility disability in community-dwelling older adults. *The Journals of Gerontology. Series A, Biological Sciences and Medical Sciences*, 62(9), 983–988. <https://doi.org/10.1093/GERONA/62.9.983>
- Braun, B. J., Veith, N. T., Hell, R., Döbele, S., Roland, M., Rollmann, M., Holstein, J., & Pohlemann, T. (2015). Validation and reliability testing of a new, fully integrated gait analysis insole. *Journal of Foot and Ankle Research*, 8(1), 1–7. <https://doi.org/10.1186/s13047-015-0111-8>
- Brown, T. N., O'Donovan, M., Hasselquist, L., Corner, B. D., & Schiffman, J. M. (2014). Body borne loads impact walk-to-run and running biomechanics. *Gait & Posture*, 40(1), 237–242. <https://doi.org/10.1016/J.GAITPOST.2014.04.001>
- Bruijn, S. M., Bregman, D. J. J., Meijer, O. G., Beek, P. J., & van Dieën, J. H. (2012). Maximum Lyapunov exponents as predictors of global gait stability: A modelling approach. *Medical Engineering & Physics*, 34(4), 428–436. <https://doi.org/10.1016/J.MEDENGGPHY.2011.07.024>
- Bruijn, S. M., Kate, W. R. T. Ten, Faber, G. S., Meijer, O. G., Beek, P. J., & Dieën, J. H. V. (2010). Estimating dynamic gait stability using data from non-aligned inertial sensors. *Annals of Biomedical Engineering*, 38(8), 2588–2593. <https://doi.org/10.1007/S10439-010-0018-2/FIGURES/4>
- Bruijn, S. M., Meijer, O. G., Beek, P. J., & Van Dieën, J. H. (2013). Assessing the stability of human locomotion: A review of current measures. *Journal of the Royal Society Interface*, 10(83). <https://doi.org/10.1098/RSIF.2012.0999>
- Bruijn, S. M., Meijer, O. G., Beek, P. J., & Van Dieën, J. H. (2010). The effects of arm swing on human gait stability. *Journal of Experimental Biology*, 213(23), 3945–3952. <https://doi.org/10.1242/JEB.045112>
- Bruijn, S. M., van Dieën, J. H., Meijer, O. G., & Beek, P. J. (2009a). Statistical precision and sensitivity of measures of dynamic gait stability. *Journal of Neuroscience Methods*, 178(2), 327–333. <https://doi.org/10.1016/J.JNEUMETH.2008.12.015>
- Bruijn, S. M., van Dieën, J. H., Meijer, O. G., & Beek, P. J. (2009b). Is slow walking more stable?

Journal of Biomechanics, 42(10), 1506–1512. <https://doi.org/10.1016/J.JBIOMECH.2009.03.047>

- Burns, G. T., Deneweth Zendler, J., & Zernicke, R. F. (2017). Wireless insoles to measure ground reaction forces: Step by step validity in hopping, walking and running. *International Society of Biomechanics Conference Proceedings*, 35 1(1), 295–298. <https://dshs-koeln.sciebo.de/index.php/s/CamALh9yXz0k6Vt>
- Callisaya, M. L., Blizzard, L., Schmidt, M. D., Martin, K. L., Mcginley, J. L., Sanders, L. M., & Srikanth, V. K. (2011). Gait, gait variability and the risk of multiple incident falls in older people: A population-based study. *Age and Ageing*, 40(4), 481–487. <https://doi.org/10.1093/AGEING/AFR055>
- Camomilla, V., Dumas, R., & Cappozzo, A. (2017). Human movement analysis: The soft tissue artefact issue. *Journal of Biomechanics*, 1–4. <https://doi.org/10.1016/j.jbiomech.2017.09.001i>
- Campaña, C. T., & Costa, P. B. (2017). Effects of walking with hand-held weights on energy expenditure and excess postexercise oxygen consumption. *Journal of Exercise Rehabilitation*, 13(6), 641. <https://doi.org/10.12965/JER.1735100.550>
- Caruso, M., Sabatini, A. M., Knaflitz, M., Gazzoni, M., Croce, U. Della, & Cereatti, A. (2021). Orientation estimation through magneto-inertial sensor fusion: A heuristic approach for suboptimal parameters tuning. *IEEE Sensors Journal*, 21(3), 3408–3419. <https://doi.org/10.1109/JSEN.2020.3024806>
- Catalfamo, P., Moser, D., Ghousayni, S., & Ewins, D. (2008). Detection of gait events using an F-Scan in-shoe pressure measurement system. *Gait and Posture*, 28(3), 420–426. <https://doi.org/10.1016/j.gaitpost.2008.01.019>
- Ceccato, J. C., de Sèze, M., Azevedo, C., & Cazalets, J. R. (2009). Comparison of trunk activity during gait initiation and walking in humans. *PLOS ONE*, 4(12), e8193. <https://doi.org/10.1371/JOURNAL.PONE.0008193>
- Ceren Ates, H., Nguyen, P. Q., Gonzalez-Macia, L., Morales-Narváez, E., Güder, F., Collins, J. J., & Dincer, C. (2022). End-to-end design of wearable sensors. *Nature Reviews Materials* 2022 7:11, 7(11), 887–907. <https://doi.org/10.1038/s41578-022-00460-x>
- Chatzaki, C., Skaramagkas, V., Tachos, N., Christodoulakis, G., Maniadi, E., Kefalopoulou, Z., Fotiadis, D. I., & Tsiknakis, M. (2021). The Smart-Insole Dataset: Gait analysis using wearable sensors with a focus on elderly and Parkinson’s patients. *Sensors*, 21(8), 1–22. <https://doi.org/10.3390/s21082821>
- Chau, T., Young, S., & Redekop, S. (2005). Managing variability in the summary and comparison of gait data. *Journal of NeuroEngineering and Rehabilitation*, 2(1), 1–20. <https://doi.org/10.1186/1743-0003-2-22/FIGURES/13>
- Chee, J. N., Ye, B., Gregor, S., Berbrayer, D., Mihailidis, A., & Patterson, K. K. (2021). Influence of multiple sclerosis on spatiotemporal gait parameters: A systematic review and meta-regression. *Archives of Physical Medicine and Rehabilitation*, 102(9), 1801–1815. <https://doi.org/10.1016/j.apmr.2020.12.013>
- Chen, D., Asaekheybari, G., Chen, H., Xu, W., & Huang, M. C. (2021). Ubiquitous fall hazard identification with smart insole. *IEEE Journal of Biomedical and Health Informatics*, 25(7), 2768–

2776. <https://doi.org/10.1109/JBHI.2020.3046701>

- Choi, S. Il, Lee, S. S., Park, H. C., & Kim, H. (2019). Gait type classification using smart insole sensors. *IEEE Region 10 Annual International Conference, Proceedings/TENCON, 2018-October*, 1903–1906. <https://doi.org/10.1109/TENCON.2018.8650147>
- Cignetti, F., Decker, L. M., & Stergiou, N. (2012). Sensitivity of the Wolf's and Rosenstein's algorithms to evaluate local dynamic stability from small gait data sets. *Annals of Biomedical Engineering*, 40(5), 1122–1130. <https://doi.org/10.1007/s10439-011-0474-3>
- Coca-Tapia, M., Cuesta-Gómez, A., Molina-Rueda, F., & Carratalá-Tejada, M. (2021). Gait pattern in people with multiple sclerosis: A systematic review. *Diagnostics*, 11(4). <https://doi.org/10.3390/DIAGNOSTICS11040584>
- Cohen, J. (1988). Statistical power analysis for the behavioral sciences. In *Statistical Power Analysis for the Behavioral Sciences* (2nd ed.). Routledge. <https://doi.org/10.4324/9780203771587>
- Collins, S. H., & Kuo, A. D. (2013). Two independent contributions to step variability during over-ground human walking. *PloS One*, 8(8). <https://doi.org/10.1371/JOURNAL.PONE.0073597>
- Cramer, L. A., Wimmer, M. A., Malloy, P., O'keefe, J. A., Knowlton, C. B., & Ferrigno, C. (2022). Validity and reliability of the Insole3 instrumented shoe insole for ground reaction force measurement during walking and running. *Sensors (Basel, Switzerland)*, 22(6). <https://doi.org/10.3390/S22062203>
- Cranage, S., Perraton, L., Bowles, K. A., & Williams, C. (2019). The impact of shoe flexibility on gait, pressure and muscle activity of young children. A systematic review. *Journal of Foot and Ankle Research*, 12(1), 1–7. <https://doi.org/10.1186/S13047-019-0365-7/TABLES/5>
- Dingwell, J. B., & Cusumano, J. P. (2000). Nonlinear time series analysis of normal and pathological human walking. *Chaos (Woodbury, N.Y.)*, 10(4), 848–863. <https://doi.org/10.1063/1.1324008>
- Dingwell, J. B., & Cusumano, J. P. (2015). Identifying stride-to-stride control strategies in human treadmill walking. *PloS One*, 10(4). <https://doi.org/10.1371/JOURNAL.PONE.0124879>
- Dingwell, J. B., Cusumano, J. P., Cavanagh, P. R., & Sternad, D. (2001). Local dynamic stability versus kinematic variability of continuous overground and treadmill walking. *Journal of Biomechanical Engineering*, 123(1), 27–32. <https://doi.org/10.1115/1.1336798>
- Dingwell, J. B., & Kang, H. G. (2007). Differences Between Local and Orbital Dynamic Stability During Human Walking. *Journal of Biomechanical Engineering*, 129(4), 586–593. <https://doi.org/10.1115/1.2746383>
- Dingwell, J. B., Kang, H. G., & Marin, L. C. (2007). The effects of sensory loss and walking speed on the orbital dynamic stability of human walking. *Journal of Biomechanics*, 40(8), 1723–1730. <https://doi.org/10.1016/J.JBIOMECH.2006.08.006>
- Dingwell, J. B., & Marin, L. C. (2006). Kinematic variability and local dynamic stability of upper body motions when walking at different speeds. *Journal of Biomechanics*, 39(3), 444–452. <https://doi.org/10.1016/J.JBIOMECH.2004.12.014>
- Dubost, V., Kressig, R. W., Gonthier, R., Herrmann, F. R., Aminian, K., Najafi, B., & Beauchet, O. (2006). Relationships between dual-task related changes in stride velocity and stride time

variability in healthy older adults. *Human Movement Science*, 25(3), 372–382.
<https://doi.org/10.1016/J.HUMOV.2006.03.004>

- Duran-Badillo, T., Salazar-González, B. C., Cruz-Quevedo, J. E., Sánchez-Alejo, E. J., Gutierrez-Sanchez, G., & Hernández-Cortés, P. L. (2020). Sensory and cognitive functions, gait ability and functionality of older adults. *Revista Latino-Americana de Enfermagem*, 28, 1–8.
<https://doi.org/10.1590/1518-8345.3499.3282>
- Eberly, L. E. (2007). Multiple linear regression. In W. T. Ambrosius (Ed.), *Topics in Biostatistics*.
- Faulkner, K. A., Cauley, J. A., Zmuda, J. M., Landsittel, D. P., Nevitt, M. C., Newman, A. B., Studenski, S. A., & Redfern, M. S. (2005). Ethnic differences in the frequency and circumstances of falling in older community-dwelling women. *Journal of the American Geriatrics Society*, 53(10), 1774–1779. <https://doi.org/10.1111/J.1532-5415.2005.53514.X>
- Ferrarello, F., Bianchi, V. A. M., Baccini, M., Rubbieri, G., Mossello, E., Cavallini, M. C., Marchionni, N., & Di Bari, M. (2013). Tools for observational gait analysis in patients with stroke: A systematic review. *Physical Therapy*, 93(12), 1673–1686. <https://doi.org/10.2522/PTJ.20120344>
- Ferrari, A., Cutti, A. G., Garofalo, P., Raggi, M., Heijboer, M., Cappello, A., & Davalli, A. (2009). First in vivo assessment of “Outwalk”: A novel protocol for clinical gait analysis based on inertial and magnetic sensors. *Medical & Biological Engineering & Computing 2009 48:1*, 48(1), 1–15.
<https://doi.org/10.1007/S11517-009-0544-Y>
- Forner-Cordero, A., Mateu-Arce, M., Forner-Cordero, I., Alcántara, E., Moreno, J. C., & Pons, J. L. (2008). Study of the motion artefacts of skin-mounted inertial sensors under different attachment conditions. *Physiological Measurement*, 29(4). <https://doi.org/10.1088/0967-3334/29/4/N01>
- Fraser, A. M., & Swinney, H. L. (1986). Independent coordinates for strange attractors from mutual information. *Physical Review A*, 33(2), 1134. <https://doi.org/10.1103/PhysRevA.33.1134>
- Fukuchi, C. A., Fukuchi, R. K., & Duarte, M. (2018). A public dataset of overground and treadmill walking kinematics and kinetics in healthy individuals. *PeerJ*, 2018(4), e4640.
<https://doi.org/10.7717/PEERJ.4640/SUPP-1>
- Fuller, J., Liu, L., Murphy, M., & Mann, R. (1997). A comparison of lower-extremity skeletal kinematics measured using skin- and pin-mounted markers. *EISEVIER Human Movement Science*, 16, 219–242.
- Gaßner, H., Jensen, D., Marxreiter, F., Kletsch, A., Bohlen, S., Schubert, R., Muratori, L. M., Eskofier, B., Klucken, J., Winkler, J., Reilmann, R., & Kohl, Z. (2020). Gait variability as digital biomarker of disease severity in Huntington’s disease. *Journal of Neurology*, 267(6), 1594–1601.
<https://doi.org/10.1007/S00415-020-09725-3/FIGURES/3>
- Gates, D. H., & Dingwell, J. B. (2009). Comparison of different state space definitions for local dynamic stability analyses. *Journal of Biomechanics*, 42(9), 1345–1349.
<https://doi.org/10.1016/J.JBIOMECH.2009.03.015>
- Hak, L., Houdijk, H., Steenbrink, F., Mert, A., Van der Wurff, P., Beek, P. J., & Van Dieën, J. H. (2012). Speeding up or slowing down?: Gait adaptations to preserve gait stability in response to balance perturbations. *Gait & Posture*, 36(2), 260–264.
<https://doi.org/10.1016/J.GAITPOST.2012.03.005>

- Hamacher, D., Hamacher, D., Singh, N. B., Taylor, W. R., & Schega, L. (2015). Towards the assessment of local dynamic stability of level-grounded walking in an older population. *Medical Engineering & Physics*, 37(12), 1152–1155. <https://doi.org/10.1016/J.MEDENGPHY.2015.09.007>
- Hamacher, D., Singh, N. B., Van Dieën, J. H., Heller, M. O., & Taylor, W. R. (2011). Kinematic measures for assessing gait stability in elderly individuals: A systematic review. *Journal of the Royal Society Interface*, 8(65), 1682. <https://doi.org/10.1098/RSIF.2011.0416>
- Hari Krishnan, R., Devanandh, V., Brahma, A. K., & Pugazhenth, S. (2016). Estimation of mass moment of inertia of human body, when bending forward, for the design of a self-transfer robotic facility. *Journal of Engineering Science and Technology*, 11(2), 166–176.
- Hausdorff, J. M. (2005). Gait variability: Methods, modeling and meaning. *Journal of NeuroEngineering and Rehabilitation*, 2(1), 1–9. <https://doi.org/10.1186/1743-0003-2-19/FIGURES/2>
- Hausdorff, J. M. (2007). Gait dynamics, fractals and falls: Finding meaning in the stride-to-stride fluctuations of human walking. *Human Movement Science*, 26(4), 555–589. <https://doi.org/10.1016/j.humov.2007.05.003>
- Hausdorff, J. M., Rios, D. A., & Edelberg, H. K. (2001). Gait variability and fall risk in community-living older adults: A 1-year prospective study. *Archives of Physical Medicine and Rehabilitation*, 82(8), 1050–1056. <https://doi.org/10.1053/APMR.2001.24893>
- Heinrich, S., Rapp, K., Rissmann, U., Becker, C., & König, H. H. (2010). Cost of falls in old age: A systematic review. *Osteoporosis International : A Journal Established as Result of Cooperation between the European Foundation for Osteoporosis and the National Osteoporosis Foundation of the USA*, 21(6), 891–902. <https://doi.org/10.1007/S00198-009-1100-1>
- Hill, A., & Nantel, J. (2019). The effects of arm swing amplitude and lower-limb asymmetry on gait stability. *PLoS ONE*, 14(12). <https://doi.org/10.1371/JOURNAL.PONE.0218644>
- Hof, A. L. (2007). The equations of motion for a standing human reveal three mechanisms for balance. *Journal of Biomechanics*, 40(2), 451–457. <https://doi.org/10.1016/J.JBIOMECH.2005.12.016>
- Holden, J. P., Orsini, J. A., Siegel, K. L., Kepple, T. M., Gerber, L. H., & Stanhope, S. J. (1997). Surface movement errors in shank kinematics and knee kinetics during gait. *Gait & Posture*, 5(3), 217–227. [https://doi.org/10.1016/S0966-6362\(96\)01088-0](https://doi.org/10.1016/S0966-6362(96)01088-0)
- Huber, P. J. (1981). *Robust Statistics*. Wiley.
- Huisinga, J. M., Schmid, K. K., Filipi, M. L., & Stergiou, N. (2013). Gait mechanics are different between healthy controls and patients with multiple sclerosis. *Journal of Applied Biomechanics*, 29(3), 303–311. <https://doi.org/10.1123/JAB.29.3.303>
- Hulleck, A. A., Menoth Mohan, D., Abdallah, N., El Rich, M., & Khalaf, K. (2022). Present and future of gait assessment in clinical practice: Towards the application of novel trends and technologies. *Frontiers in Medical Technology*, 4, 901331. <https://doi.org/10.3389/FMEDT.2022.901331/BIBTEX>
- Ihlen, E. A. F., van Schooten, K. S., Bruijn, S. M., Pijnappels, M., & van Dieën, J. H. (2017). Fractional stability of trunk acceleration dynamics of daily-life walking: Toward a unified concept of gait stability. *Frontiers in Physiology*, 8(AUG), 516.

<https://doi.org/10.3389/FPHYS.2017.00516/BIBTEX>

- Ihlen, E. A. F., Weiss, A., Beck, Y., Helbostad, J. L., & Hausdorff, J. M. (2016). A comparison study of local dynamic stability measures of daily life walking in older adult community-dwelling fallers and non-fallers. *Journal of Biomechanics*, *49*(9), 1498–1503. <https://doi.org/10.1016/J.JBIOMECH.2016.03.019>
- Jonsson, H., & Kärrholm, J. (1994). Three-dimensional knee joint movements during a step-up: Evaluation after anterior cruciate ligament rupture. *Journal of Orthopaedic Research*, *12*(6), 769–779. <https://doi.org/10.1002/JOR.1100120604>
- Kamm, K., Thelen, E., & Jensen, J. L. (1990). A dynamical systems approach to motor development. *Physical Therapy*, *70*(12), 763–775. <https://doi.org/10.1093/ptj/70.12.763>
- Kang, H. G., & Dingwell, J. B. (2006). A direct comparison of local dynamic stability during unperturbed standing and walking. *Experimental Brain Research*, *172*(1), 35–48. <https://doi.org/10.1007/s00221-005-0224-6>
- Kang, H. G., & Dingwell, J. B. (2008). Separating the effects of age and walking speed on gait variability. *Gait & Posture*, *27*, 572–577. <https://doi.org/10.1016/j.gaitpost.2007.07.009>
- Kang, H. G., & Dingwell, J. B. (2009). Dynamic stability of superior vs. inferior segments during walking in young and older adults. *Gait & Posture*, *30*(2), 260–263. <https://doi.org/10.1016/J.GAITPOST.2009.05.003>
- Kanko, R., Laende, E., Selbie, W. S., & Deluzio, K. J. (2021). Inter-session repeatability of markerless motion capture gait kinematics. *Journal of Biomechanics*, *121*, 110422. <https://doi.org/10.1016/J.JBIOMECH.2021.110422>
- Kanko, R., Strutzenberger, G., Brown, M., Selbie, S., & Deluzio, K. (2021). Assessment of spatiotemporal gait parameters using a deep learning algorithm-based markerless motion capture system. *Journal of Biomechanics*. <https://doi.org/10.31224/osf.io/j4rbg>
- Karthikbabu, S., Rao, B. K., Manikandan, N., Solomon, J. M., Chakrapani, M., & Nayak, A. (2011). Role of trunk rehabilitation on trunk control, balance and gait in patients with chronic stroke: A pre-post design. *Neuroscience & Medicine*, *2011*(02), 61–67. <https://doi.org/10.4236/NM.2011.22009>
- Kennel, M. B., Brown, R., & Abarbanel, H. D. I. (1992). Determining embedding dimension for phase-space reconstruction using a geometrical construction. *Physical Review A*, *45*(6), 3403. <https://doi.org/10.1103/PhysRevA.45.3403>
- Kharb, A., Saini, V., Jain, Y., & Dhiman, S. (2011). A review of gait cycle and its parameters. *IJCEM Int J Comput Eng Manag*, *13*(July), 78–83.
- Kluger, D., Major, M. J., Fatone, S., & Gard, S. A. (2014). The effect of trunk flexion on lower-limb kinetics of able-bodied gait [Article]. *Human Movement Science*, *33*, 395–403. <https://doi.org/10.1016/j.humov.2013.12.006>
- Kobsar, D., Charlton, J. M., Tse, C. T. F., Esculier, J. F., Graffos, A., Krowchuk, N. M., Thatcher, D., & Hunt, M. A. (2020). Validity and reliability of wearable inertial sensors in healthy adult walking: A systematic review and meta-analysis. *Journal of NeuroEngineering and Rehabilitation* *2020* *17*:1, *17*(1), 1–21. <https://doi.org/10.1186/S12984-020-00685-3>

- Kok, M., Hol, J. D., & Schön, T. B. (2017). Using inertial sensors for position and orientation estimation. *Foundations and Trends in Signal Processing*, *11*(1–2), 1–153. <https://doi.org/10.1561/20000000094>
- König, N., Taylor, W. R., Baumann, C. R., Wenderoth, N., & Singh, N. B. (2016). Revealing the quality of movement: A meta-analysis review to quantify the thresholds to pathological variability during standing and walking. *Neuroscience & Biobehavioral Reviews*, *68*, 111–119. <https://doi.org/10.1016/J.NEUBIOREV.2016.03.035>
- Koo, T. K., & Li, M. Y. (2016). A guideline of selecting and reporting intraclass correlation coefficients for reliability research. *Journal of Chiropractic Medicine*, *15*(2), 155–163. <https://doi.org/10.1016/j.jcm.2016.02.012>
- Krakovská, A., Mezeiová, K., & Budáčová, H. (2015). Use of false nearest neighbours for selecting variables and embedding parameters for state space reconstruction. *Journal of Complex Systems*, *2015*, 1–12. <https://doi.org/10.1155/2015/932750>
- Kroneberg, D., Elshehabi, M., Meyer, A. C., Otte, K., Doss, S., Paul, F., Nussbaum, S., Berg, D., Kühn, A. A., Maetzler, W., & Schmitz-Hübsch, T. (2019). Less is more - Estimation of the number of strides required to assess gait variability in spatially confined settings. *Frontiers in Aging Neuroscience*, *11*(JAN), 389096. <https://doi.org/10.3389/FNAGI.2018.00435/BIBTEX>
- Kumar, S. (2004). Ergonomics and biology of spinal rotation. *Ergonomics*, *47*(4), 370–415. <https://doi.org/10.1080/0014013032000157940>
- Lamb, S. E., Jørstad-Stein, E. C., Hauer, K., & Becker, C. (2005). Development of a common outcome data set for fall injury prevention trials: The Prevention of Falls Network Europe consensus. *Journal of the American Geriatrics Society*, *53*(9), 1618–1622. <https://doi.org/10.1111/J.1532-5415.2005.53455.X>
- Larsen, W. A., & McCleary, S. J. (1972). The use of partial residual plots in regression analysis. *Technometrics*, *14*(3), 781. <https://doi.org/10.2307/1267305>
- Laudanski, A., Brouwer, B., & Li, Q. (2013). Measurement of lower limb joint kinematics using inertial sensors during stair ascent and descent in healthy older adults and stroke survivors. *Journal of Healthcare Engineering*, *4*(4), 555–576. <https://doi.org/10.1260/2040-2295.4.4.555>
- Lee, H. S., Lee, J. H., & Kim, H. S. (2019). Activities of ankle muscles during gait analyzed by simulation using the human musculoskeletal model. *Journal of Exercise Rehabilitation*, *15*(2), 229. <https://doi.org/10.12965/JER.1938054.027>
- Lee, J., Kim, D., Ryoo, H. Y., & Shin, B. S. (2016). Sustainable wearables: Wearable technology for enhancing the quality of human life. *Sustainability 2016, Vol. 8, Page 466*, *8*(5), 466. <https://doi.org/10.3390/SU8050466>
- Lewis, J. E., & Neider, M. B. (2017). Designing Wearable Technology for an Aging Population. *Ergonomics in Design*, *25*(3), 4–10. <https://doi.org/10.1177/1064804616645488>
- Ligorio, G., Bergamini, E., Pasciuto, I., Vannozzi, G., Cappozzo, A., & Sabatini, A. M. (2016). Assessing the performance of sensor fusion methods: Application to magnetic-inertial-based human body tracking. *Sensors 2016, Vol. 16, Page 153*, *16*(2), 153. <https://doi.org/10.3390/S16020153>
- Lin, D., Papi, E., & McGregor, A. H. (2019). Exploring the clinical context of adopting an instrumented

- insole: A qualitative study of clinicians' preferences in England. *BMJ Open*, 9(4), e023656. <https://doi.org/10.1136/BMJOPEN-2018-023656>
- Liu, Jian, Zhang, X., & Lockhart, T. E. (2012). Fall risk assessments based on postural and dynamic stability using inertial measurement unit. *Safety and Health at Work*, 3(3), 192. <https://doi.org/10.5491/SHAW.2012.3.3.192>
- Liu, Jinyuan, Tang, W., Chen, G., Lu, Y., Feng, C., & Tu, X. M. (2016). Correlation and agreement: Overview and clarification of competing concepts and measures. *Shanghai Archives of Psychiatry*, 28(2), 115. <https://doi.org/10.11919/J.ISSN.1002-0829.216045>
- Lockhart, T. E., & Liu, J. (2008). Differentiating fall-prone and healthy adults using local dynamic stability. *Ergonomics*, 51(12), 1860. <https://doi.org/10.1080/00140130802567079>
- Longo, A., Federolf, P., Haid, T., & Meulenbroek, R. (2018). Effects of a cognitive dual task on variability and local dynamic stability in sustained repetitive arm movements using principal component analysis: A pilot study. *Experimental Brain Research*, 236(6), 1611–1619. <https://doi.org/10.1007/S00221-018-5241-3/FIGURES/4>
- Lord, S. E., & Rochester, L. (2005). Measurement of community ambulation after stroke. *Stroke*, 36(7), 1457–1461. <https://doi.org/10.1161/01.STR.0000170698.20376.2E>
- Lugade, V., Lin, V., & Chou, L. S. (2011). Center of mass and base of support interaction during gait. *Gait & Posture*, 33(3), 406–411. <https://doi.org/10.1016/J.GAITPOST.2010.12.013>
- Lyapunov, A. M. (1992). The general problem of the stability of motion. *International Journal of Control*, 55(3), 531–534. <https://doi.org/10.1080/00207179208934253>
- Ma, L., Mi, T. M., Jia, Q., Han, C., Chhetri, J. K., & Chan, P. (2022). Gait variability is sensitive to detect Parkinson's disease patients at high fall risk. *The International Journal of Neuroscience*, 132(9), 888–893. <https://doi.org/10.1080/00207454.2020.1849189>
- Madgwick, S. O. H., Harrison, A. J. L., & Vaidyanathan, R. (2011). Estimation of IMU and MARG orientation using a gradient descent algorithm. *IEEE International Conference on Rehabilitation Robotics*. <https://doi.org/10.1109/ICORR.2011.5975346>
- Maki, B. E. (1997). Gait changes in older adults: Predictors of falls or indicators of fear? *Journal of the American Geriatrics Society*, 45(3), 313–320. <https://doi.org/10.1111/J.1532-5415.1997.TB00946.X>
- Marill, K. A. (2004a). Advanced statistics: Linear regression, Part I: Simple linear regression. *Academic Emergency Medicine*, 11(1), 87–93. <https://doi.org/10.1197/J.AEM.2003.09.005>
- Marill, K. A. (2004b). Advanced statistics: Linear regression, Part II: Multiple linear regression. *Academic Emergency Medicine*, 11(1), 94–102. <https://doi.org/10.1197/J.AEM.2003.09.006>
- Mavor, M. P., Ross, G. B., Clouthier, A. L., Karakolis, T., & Graham, R. B. (2020). Validation of an IMU suit for military-based tasks. *Sensors*, 20(15), 1–14. <https://doi.org/10.3390/s20154280>
- McAndrew, P. M., Wilken, J. M., & Dingwell, J. B. (2011). Dynamic stability of human walking in visually and mechanically destabilizing environments. *Journal of Biomechanics*, 44(4), 644–649. <https://doi.org/10.1016/J.JBIOMECH.2010.11.007>

- McArdle, R., Del Din, S., Donaghy, P., Galna, B., Thomas, A. J., & Rochester, L. (2021). The impact of environment on gait assessment: Considerations from real-world gait analysis in dementia subtypes. *Sensors (Basel, Switzerland)*, *21*(3), 1–15. <https://doi.org/10.3390/S21030813>
- McGraw, K. O., & Wong, S. P. (1996). Forming inferences about some intraclass correlation coefficients. *Psychological Methods*, *1*(1), 30–46. <https://doi.org/10.1037/1082-989X.1.1.30>
- Menéndez, A. F., Saubade, M., Hans, D., Millet, G. P., & Malatesta, D. (2019). The determinants of the preferred walking speed in individuals with obesity. *Obesity Facts*, *12*(5), 543. <https://doi.org/10.1159/000501968>
- Merriau, P., Dupuis, Y., Bouteau, R., Vasseur, P., & Savatier, X. (2017). A study of Vicon system positioning performance. *Sensors*, *17*(7), 1591. <https://doi.org/10.3390/s17071591>
- Mertz, K. J., Lee, D. chul, Sui, X., Powell, K. E., & Blair, S. N. (2010). Falls among adults: The association of cardiorespiratory fitness and physical activity with walking-related falls. *American Journal of Preventive Medicine*, *39*(1), 15. <https://doi.org/10.1016/J.AMEPRE.2010.03.013>
- Michalak, J., Troje, N. F., Rer Nat, D., Fischer, J., Vollmar, P., Heidenreich, T., & Schulte, D. (2009). Embodiment of sadness and depression - Gait patterns associated with dysphoric mood. *Psychosomatic Medicine*, *71*(5), 580–587. <https://doi.org/10.1097/PSY.0b013e3181a2515c>
- Middleton, A., Fritz, S. L., & Lusardi, M. (2015). Walking speed: The functional vital sign. *Journal of Aging and Physical Activity*, *23*(2), 314–322. <https://doi.org/10.1123/JAPA.2013-0236>
- Mirelman, A., Shema, S., Maidan, I., & Hausdorff, J. M. (2018). Gait. *Handbook of Clinical Neurology*, *159*, 119–134. <https://doi.org/10.1016/B978-0-444-63916-5.00007-0>
- Moe-Nilssen, R. (1998). A new method for evaluating motor control in gait under real-life environmental conditions. Part 2: Gait analysis. *Clinical Biomechanics*, *13*, 328–335.
- Moe-Nilssen, R., & Helbostad, J. L. (2005). Interstride trunk acceleration variability but not step width variability can differentiate between fit and frail older adults. *Gait and Posture*, *21*(2), 164–170. <https://doi.org/10.1016/j.gaitpost.2004.01.013>
- Mohamed Refai, M. I., van Beijnum, B. J. F., Buurke, J. H., & Veltink, P. H. (2019). Gait and dynamic balance sensing using wearable foot sensors. *IEEE Transactions on Neural Systems and Rehabilitation Engineering : A Publication of the IEEE Engineering in Medicine and Biology Society*, *27*(2), 218–227. <https://doi.org/10.1109/TNSRE.2018.2885309>
- Moon, Y., Sung, J. H., An, R., Hernandez, M. E., & Sosnoff, J. J. (2016). Gait variability in people with neurological disorders: A systematic review and meta-analysis. *Human Movement Science*, *47*, 197–208. <https://doi.org/10.1016/J.HUMOV.2016.03.010>
- Moon, Y., Wajda, D. A., Motl, R. W., & Sosnoff, J. J. (2015). Stride-time variability and fall risk in persons with multiple sclerosis. *Multiple Sclerosis International*, *2015*, 1–7. <https://doi.org/10.1155/2015/964790>
- Morris, R., Lord, S., Bunce, J., Burn, D., & Rochester, L. (2016). Gait and cognition: Mapping the global and discrete relationships in ageing and neurodegenerative disease. *Neuroscience and Biobehavioral Reviews*, *64*, 326–345. <https://doi.org/10.1016/J.NEUBIOREV.2016.02.012>
- Motha, L., Kim, J., & Kim, W. S. (2015). Instrumented rubber insole for plantar pressure sensing.

Organic Electronics, 23, 82–86. <https://doi.org/10.1016/J.ORGEL.2015.04.020>

- Murray, M. P., Spurr, G. B., Sepic, S. B., Gardner, G. M., & Mollinger, L. A. (1985). Treadmill vs. floor walking: Kinematics, electromyogram, and heart rate. *Journal of Applied Physiology*, 59(1), 87–91. <https://doi.org/10.1152/JAPPL.1985.59.1.87>
- Mustufa, Y. S. A., Barton, J., O’Flynn, B., Davies, R., McCullagh, P., & Zheng, H. (2015). Design of a smart insole for ambulatory assessment of gait. *2015 IEEE 12th International Conference on Wearable and Implantable Body Sensor Networks, BSN 2015*. <https://doi.org/10.1109/BSN.2015.7299383>
- Nagano, H., Sarashina, E., Sparrow, W., Mizukami, K., & Begg, R. (2019). General mental health is associated with gait asymmetry. *Sensors (Basel, Switzerland)*, 19(22). <https://doi.org/10.3390/S19224908>
- Novak, D., & Riener, R. (2015). A survey of sensor fusion methods in wearable robotics. *Robotics and Autonomous Systems*, 73, 155–170. <https://doi.org/10.1016/J.ROBOT.2014.08.012>
- Nymark, J. R., Balmer, S. J., Melis, E. H., Lemaire, E. D., & Millar, S. (2005). Electromyographic and kinematic nondisabled gait differences at extremely slow overground and treadmill walking speeds. *Journal of Rehabilitation Research and Development*, 42(4), 523–534. <https://doi.org/10.1682/JRRD.2004.05.0059>
- Oerbekke, M. S., Stukstette, M. J., Schütte, K., de Bie, R. A., Pisters, M. F., & Vanwanseele, B. (2017). Concurrent validity and reliability of wireless instrumented insoles measuring postural balance and temporal gait parameters. *Gait & Posture*, 51, 116–124. <https://doi.org/10.1016/J.GAITPOST.2016.10.005>
- Ortega, J. D., Fehlman, L. A., & Farley, C. T. (2008). Effects of aging and arm swing on the metabolic cost of stability in human walking. *Journal of Biomechanics*, 41(16), 3303. <https://doi.org/10.1016/J.JBIOMECH.2008.06.039>
- Owings, T. M., & Grabiner, M. D. (2003). Measuring step kinematic variability on an instrumented treadmill: How many steps are enough? *Journal of Biomechanics*, 36(8), 1215–1218. [https://doi.org/10.1016/S0021-9290\(03\)00108-8](https://doi.org/10.1016/S0021-9290(03)00108-8)
- Pearson, C., St-Arnaud, J., & Geran, L. (2014). *Understanding seniors’ risk of falling and their perception of risk Health at a Glance*. www.statcan.gc.ca,
- Pedro, B., Cabral, S., & Veloso, A. P. (2021). Concurrent validity of an inertial measurement system in tennis forehand drive. *Journal of Biomechanics*, 121, 110410. <https://doi.org/10.1016/J.JBIOMECH.2021.110410>
- Phelan, E. A., Mahoney, J. E., Voit, J. C., & Stevens, J. A. (2015). Assessment and management of fall risk in primary care settings. *The Medical Clinics of North America*, 99(2), 281. <https://doi.org/10.1016/J.MCNA.2014.11.004>
- Pirker, W., & Katzenschlager, R. (2017). Gait disorders in adults and the elderly: A clinical guide. *Wiener Klinische Wochenschrift*, 129(3), 81. <https://doi.org/10.1007/S00508-016-1096-4>
- Punt, M., Bruijn, S. M., Wittink, H., & van Dieën, J. H. (2015). Effect of arm swing strategy on local dynamic stability of human gait. *Gait & Posture*, 41(2), 504–509. <https://doi.org/10.1016/J.GAITPOST.2014.12.002>

- Raffalt, P. C., Senderling, B., & Stergiou, N. (2020). Filtering affects the calculation of the largest Lyapunov exponent. *Computers in Biology and Medicine*, *122*, 103786. <https://doi.org/10.1016/J.COMPBIOMED.2020.103786>
- Rammer, J., Slavens, B., Krzak, J., Winters, J., Riedel, S., & Harris, G. (2018). Assessment of a markerless motion analysis system for manual wheelchair application. *Journal of NeuroEngineering and Rehabilitation*, *15*(1), 96. <https://doi.org/10.1186/s12984-018-0444-1>
- Rantalainen, T., Pirkola, H., Karavirta, L., Rantanen, T., & Linnamo, V. (2019). Reliability and concurrent validity of spatiotemporal stride characteristics measured with an ankle-worn sensor among older individuals. *Gait and Posture*, *74*(April), 33–39. <https://doi.org/10.1016/j.gaitpost.2019.08.006>
- Ratner, B. (2009). The correlation coefficient: Its values range between 1/1, or do they. *Journal of Targeting, Measurement and Analysis for Marketing*, *17*(2), 139–142. <https://doi.org/10.1057/jt.2009.5>
- Remelius, J. G., Hamill, J., & van Emmerik, R. E. A. (2014). Prospective dynamic balance control during the swing phase of walking: Stability boundaries and time-to-contact analysis. *Human Movement Science*, *36*, 227–245. <https://doi.org/10.1016/J.HUMOV.2014.04.001>
- Riley, P. O., Paolini, G., Della Croce, U., Paylo, K. W., & Kerrigan, D. C. (2007). A kinematic and kinetic comparison of overground and treadmill walking in healthy subjects. *Gait & Posture*, *26*(1), 17–24. <https://doi.org/10.1016/J.GAITPOST.2006.07.003>
- Rispens, S. M., Van Schooten, K. S., Pijnappels, M., Daffertshofer, A., Beek, P. J., & Van Dieën, J. H. (2015). Identification of fall risk predictors in daily life measurements: Gait characteristics' reliability and association with self-reported fall history. *Neurorehabilitation and Neural Repair*, *29*(1), 54–61. https://doi.org/10.1177/1545968314532031/ASSET/IMAGES/LARGE/10.1177_1545968314532031-FIG1.JPEG
- Rosati, S., Ghislieri, M., Dotti, G., Fortunato, D., Agostini, V., Knaflitz, M., & Balestra, G. (2021). Evaluation of muscle function by means of a muscle-specific and a global index. *Sensors (Basel, Switzerland)*, *21*(21). <https://doi.org/10.3390/S21217186>
- Rosenstein, M. T., Collins, J. J., & De Luca, C. J. (1993). A practical method for calculating largest Lyapunov exponents from small data sets. *Physica D: Nonlinear Phenomena*, *65*(1–2), 117–134. [https://doi.org/10.1016/0167-2789\(93\)90009-P](https://doi.org/10.1016/0167-2789(93)90009-P)
- Roth, N., Martindale, C. F., Gaßner, H., Kohl, Z., Klucken, J., & Eskofer, B. M. (2018). Synchronized sensor insoles for clinical gait analysis in home-monitoring applications. *Current Directions in Biomedical Engineering*, *4*(1), 433–437. <https://doi.org/10.1515/CDBME-2018-0103/MACHINEREADABLECITATION/RIS>
- Saber-Sheikh, K., Bryant, E. C., Glazzard, C., Hamel, A., & Lee, R. Y. W. (2010). Feasibility of using inertial sensors to assess human movement. *Manual Therapy*, *15*(1), 122–125. <https://doi.org/10.1016/J.MATH.2009.05.009>
- Sardoğan, C., Muammer, R., Akalan, N. E., Sert, R., & Bilgili, F. (2021). Determining the relationship between the impairment of selective voluntary motor control and gait deviations in children with cerebral palsy using simple video-based analyses. *Gait & Posture*, *90*, 295–300.

<https://doi.org/10.1016/J.GAITPOST.2021.08.019>

- Sato, S. D., Hiroi, Y., Zoppo, D., Buonaccorsi, J., Miehm, J. D., & van Emmerik, R. E. A. (2022). Spatiotemporal gait changes in people with multiple sclerosis with different disease progression subtypes. *Clinical Biomechanics (Bristol, Avon)*, *100*.
<https://doi.org/10.1016/J.CLINBIOMECH.2022.105818>
- Schmitt, A. C., Baudendistel, S. T., Fallon, M. S., Roper, J. A., & Hass, C. J. (2020). Assessing the relationship between the enhanced gait variability index and falls in individuals with Parkinson's disease. *Parkinson's Disease*, *2020*. <https://doi.org/10.1155/2020/5813049>
- Schmitt, A. C., Baudendistel, S. T., Lipat, A. L., White, T. A., Raffegeau, T. E., & Hass, C. J. (2021). Walking indoors, outdoors, and on a treadmill: Gait differences in healthy young and older adults. *Gait & Posture*, *90*, 468–474. <https://doi.org/10.1016/J.GAITPOST.2021.09.197>
- Scholz, J. P., & Schöner, G. (1999). The uncontrolled manifold concept: Identifying control variables for a functional task. *Experimental Brain Research*, *126*(3), 289–306.
<https://doi.org/10.1007/s002210050738>
- Schwartz, M. H., Trost, J. P., & Werve, R. A. (2004). Measurement and management of errors in quantitative gait data. *Gait & Posture*, *20*(2), 196–203.
<https://doi.org/10.1016/J.GAITPOST.2003.09.011>
- Sekine, M., Tamura, T., Yoshida, M., Suda, Y., Kimura, Y., Miyoshi, H., Kijima, Y., Higashi, Y., & Fujimoto, T. (2013). A gait abnormality measure based on root mean square of trunk acceleration. *Journal of NeuroEngineering and Rehabilitation*, *10*(1), 1–7. <https://doi.org/10.1186/1743-0003-10-118/FIGURES/5>
- Shah, V. V., McNames, J., Mancini, M., Carlson-Kuhta, P., Spain, R. I., Nutt, J. G., El-Gohary, M., Curtze, C., & Horak, F. B. (2020). Laboratory versus daily life gait characteristics in patients with multiple sclerosis, Parkinson's disease, and matched controls. *Journal of NeuroEngineering and Rehabilitation*, *17*(1), 1–12. <https://doi.org/10.1186/S12984-020-00781-4/FIGURES/4>
- Simpson, S. H. (2015). Creating a data analysis plan: What to consider when choosing statistics for a study. *The Canadian Journal of Hospital Pharmacy*, *68*(4), 311.
<https://doi.org/10.4212/CJHP.V68I4.1471>
- Sloot, L. H., Van Schooten, K. S., Bruijn, S. M., Kingma, H., Pijnappels, M., & Van Dieën, J. H. (2011). Sensitivity of local dynamic stability of over-ground walking to balance impairment due to galvanic vestibular stimulation. *Annals of Biomedical Engineering*, *39*(5), 1563.
<https://doi.org/10.1007/S10439-010-0240-Y>
- Socie, M. J., Motl, R. W., Pula, J. H., Sandroff, B. M., & Sosnoff, J. J. (2013). Gait variability and disability in multiple sclerosis. *Gait and Posture*, *38*(1), 51–55.
<https://doi.org/10.1016/j.gaitpost.2012.10.012>
- Socie, M. J., & Sosnoff, J. J. (2013). Gait variability and multiple sclerosis. *Multiple Sclerosis International*, *2013*, 1–7. <https://doi.org/10.1155/2013/645197>
- Song, J. L., & Hidler, J. (2008). Biomechanics of overground vs. treadmill walking in healthy individuals. *Journal of Applied Physiology*, *104*(3), 747–755.
<https://doi.org/10.1152/JAPPLPHYSIOL.01380.2006/ASSET/IMAGES/LARGE/ZDG0020877150>

004.JPEG

- Sorrentino, I., Chavez, F. J. A., Latella, C., Fiorio, L., Traversaro, S., Rapetti, L., Tirupachuri, Y., Guedelha, N., Maggiali, M., Dussoni, S., Metta, G., & Pucci, D. (2020). A novel sensorised insole for sensing feet pressure distributions. *Sensors 2020, Vol. 20, Page 747, 20(3), 747*.
<https://doi.org/10.3390/S20030747>
- Sparrow, W. A., & Newell, K. M. (1994). The coordination and control of human creeping with increases in speed. *Behavioural Brain Research, 63(2), 151–158*. [https://doi.org/10.1016/0166-4328\(94\)90086-8](https://doi.org/10.1016/0166-4328(94)90086-8)
- Spörri, J., Schiefermüller, C., & Müller, E. (2016). Collecting kinematic data on a ski track with optoelectronic stereophotogrammetry: A methodological study assessing the feasibility of bringing the biomechanics lab to the field. *PLOS ONE, 11(8), e0161757*.
<https://doi.org/10.1371/journal.pone.0161757>
- Statistics Canada. (2022, August 22). *Population Projections for Canada, Provinces and Territories, 2021 to 2068, 2022*. The Daily. <https://www150.statcan.gc.ca/n1/daily-quotidien/220822/dq220822b-eng.htm>
- Stergiou, N., & Decker, L. M. (2011). Human movement variability, nonlinear dynamics, and pathology: Is there a connection? *Human Movement Science, 30(5), 869–888*.
<https://doi.org/10.1016/j.humov.2011.06.002>
- Stergiou, N., Harbourne, R. T., & Cavanaugh, J. T. (2006). Optimal movement variability: A new theoretical perspective for neurologic physical therapy. *Journal of Neurologic Physical Therapy, 30(3), 120–129*. <https://doi.org/10.1097/01.NPT.0000281949.48193.D9>
- Stöggel, T., & Martinier, A. (2016). Validation of Moticon's OpenGo sensor insoles during gait, jumps, balance and cross-country skiing specific imitation movements.
<https://doi.org/10.1080/02640414.2016.1161205>, *35(2), 196–206*.
<https://doi.org/10.1080/02640414.2016.1161205>
- Strimbu, K., & Tavel, J. A. (2010). What are Biomarkers? *Current Opinion in HIV and AIDS, 5(6), 463*.
<https://doi.org/10.1097/COH.0B013E32833ED177>
- Su, J. L. S., & Dingwell, J. B. (2007). Dynamic stability of passive Dynamic walking on an irregular surface. *Journal of Biomechanical Engineering, 129(6), 802–810*.
<https://doi.org/10.1115/1.2800760>
- Subramaniam, S., Majumder, S., Faisal, A. I., & Jamal Deen, M. (2022). Insole-based systems for health monitoring: Current solutions and research challenges. *Sensors 2022, Vol. 22, Page 438, 22(2), 438*. <https://doi.org/10.3390/S22020438>
- Summers, J. J., & Anson, J. G. (2009). Current status of the motor program: revisited. *Human Movement Science, 28(5), 566–577*. <https://doi.org/10.1016/J.HUMOV.2009.01.002>
- Tao, W., Liu, T., Zheng, R., & Feng, H. (2012). Gait analysis using wearable sensors. *Sensors (Basel, Switzerland), 12(2), 2255*. <https://doi.org/10.3390/S120202255>
- Terrier, P., & Dériaz, O. (2011). Kinematic variability, fractal dynamics and local dynamic stability of treadmill walking. *Journal of NeuroEngineering and Rehabilitation, 8(1), 1–14*.
<https://doi.org/10.1186/1743-0003-8-12/TABLES/3>

- Terrier, P., & Reynard, F. (2015). Effect of age on the variability and stability of gait: A cross-sectional treadmill study in healthy individuals between 20 and 69 years of age. *Gait & Posture*, *41*(1), 170–174. <https://doi.org/10.1016/J.GAITPOST.2014.09.024>
- Toebes, M. J. P., Hoozemans, M. J. M., Furrer, R., Dekker, J., & Van Dieën, J. H. (2012). Local dynamic stability and variability of gait are associated with fall history in elderly subjects. *Gait & Posture*, *36*(3), 527–531. <https://doi.org/10.1016/J.GAITPOST.2012.05.016>
- Tranmer, M., Murphy, J., Elliot, M., & Pampaka, M. (2020). *Multiple Linear Regression (2 nd Edition)*. <https://hummedia.manchester.ac.uk/institutes/cmist/a>
- Trunfio, T. A., Scala, A., Giglio, C., Rossi, G., Borrelli, A., Romano, M., & Improta, G. (2022). Multiple regression model to analyze the total LOS for patients undergoing laparoscopic appendectomy. *BMC Medical Informatics and Decision Making*, *22*(1). <https://doi.org/10.1186/S12911-022-01884-9>
- Umberger, B. R. (2010). Stance and swing phase costs in human walking. *Journal of the Royal Society Interface*, *7*(50), 1329. <https://doi.org/10.1098/RSIF.2010.0084>
- Vaapio, S. S., Salminen, M. J., Ojanlatva, A., & Kivelä, S. L. (2009). Quality of life as an outcome of fall prevention interventions among the aged: A systematic review. *European Journal of Public Health*, *19*(1), 7–15. <https://doi.org/10.1093/EURPUB/CKN099>
- Van Hooren, B., Willems, P., Plasqui, G., & Meijer, K. (2023). The accuracy of commercially available instrumented insoles (ARION) for measuring spatiotemporal running metrics. *Scandinavian Journal of Medicine & Science in Sports*. <https://doi.org/10.1111/SMS.14424>
- van Schooten, K. S., Rispens, S. M., Pijnappels, M., Daffertshofer, A., & van Dieën, J. H. (2013). Assessing gait stability: The influence of state space reconstruction on inter- and intra-day reliability of local dynamic stability during over-ground walking. *Journal of Biomechanics*, *46*(1), 137–141. <https://doi.org/10.1016/J.JBIOMECH.2012.10.032>
- Verghese, J., Holtzer, R., Lipton, R. B., & Wang, C. (2009). Quantitative gait markers and incident fall risk in older adults. *The Journals of Gerontology Series A: Biological Sciences and Medical Sciences*, *64A*(8), 896. <https://doi.org/10.1093/GERONA/GLP033>
- Watt, J. R., Franz, J. R., Jackson, K., Dicharry, J., Riley, P. O., & Kerrigan, D. C. (2010). A three-dimensional kinematic and kinetic comparison of overground and treadmill walking in healthy elderly subjects. *Clinical Biomechanics*, *25*(5), 444–449. <https://doi.org/10.1016/J.CLINBIOMECH.2009.09.002>
- Williams, D. (2020). *Investigating how the double support period affects fall risk in bipedal gait* (Issue December). Pennsylvania State University.
- Winter, D. A. (1995). Human balance and posture control during standing and walking. *Gait & Posture*, *3*, 193–214.
- Wolf, A., Swift, J. B., Swinney, H. L., & Vastano, J. A. (1985). Determining Lyapunov exponents from a time series. *Physica D: Nonlinear Phenomena*, *16*(3), 285–317. [https://doi.org/10.1016/0167-2789\(85\)90011-9](https://doi.org/10.1016/0167-2789(85)90011-9)
- Xsens Technologies B.V. (2021). MVN User Manual. *MVN Manual*, April, 162. <https://www.cleancss.com/user-manuals/QIL/MTW2-3A7G6>

- Yang, F., & King, G. A. (2016). Dynamic gait stability of treadmill versus overground walking in young adults. *Journal of Electromyography and Kinesiology*, *31*, 81–87.
<https://doi.org/10.1016/J.JELEKIN.2016.09.004>
- Zhang, J. T., Novak, A. C., Brouwer, B., & Li, Q. (2013). Concurrent validation of Xsens MVN measurement of lower limb joint angular kinematics. *Physiological Measurement*, *34*(8), N63.
<https://doi.org/10.1088/0967-3334/34/8/N63>



Université d'Ottawa
Faculté des sciences
de la santé

École des sciences de
l'activité physique

University of Ottawa
Faculty of Health
Sciences

School of Human
Kinetics

Appendix A: Research Consent Form Research Consent Form

Research Project Title: Development of a gait detection algorithm for individuals with multiple sclerosis

Principal Investigator: Dr. Ryan Graham¹

Research Assistants: Matthew Mavor¹,
Alexandre Mir-Orifice¹

¹University of Ottawa, Faculty of Health Sciences, Department of Human Kinetics, 200 Lees Ave (E020), Ottawa, ON K1N6N5

COVID-19 Precautions:

For the safety of both yourself and the researchers, precautions have been put in place to try and prevent the spread of COVID-19. Before arriving at the lab, you and the researchers will be screened for COVID-19 symptoms and will be asked to use hand sanitizer upon entering and exiting the lab. Both you and the researchers are required to wear a mask at all times during the data collection as well as protective eyewear. All equipment that is touched by either a participant or a researcher during the collection will be wiped down with disinfectant before and after the collection and all washable materials will be washed in between each participant starting. There will be a mandatory minimum of 30 minutes between data collections.

Background and Purpose of the Study:

Multiple sclerosis (MS) is an inflammatory-based disease that causes demyelination of the central nervous system tissues. People with MS experience a variety of neurological impairments, the most common of which is to their gait. Due to the nature of MS, gait impairments are highly variable resulting in no “common” gait pattern among this population. Since gait is often used as a clinical identifier for the progression of MS, it is imperative that we understand how individuals walk on a personal level so we can track their progression and inform their clinicians with objective information so appropriate medical and exercise interventions can be administered.

There has been a large recent shift towards wearable sensor technology to track human movement outside of the laboratory environment. Two of these technologies are inertial measurement units (IMUs), which are small sensors that measure linear acceleration, angular velocity, and the magnetic field, and instrumented smart insoles that measure pressure and linear acceleration. In order to effectively deploy these technologies in the field, we must first develop methods to identify common human activities. In partnership with Wesley Clover International, our purpose is to develop intellectual property using IMUs and smart insoles to identify parameters of several gait parameters (e.g., step length, step width, stance time, and walking speed) to develop personalized models that characterize individuals’ gait parameter to track the progression of MS.

☎ 613-562-5853
☎ 613-562-5149

125 University Private
Ottawa ON K1N 6N5 Canada

www.uOttawa.ca

Description of Study Procedures:

You are invited to participate in a one-day motion analysis procedure for approximately 1 hour and the University of Ottawa Spine and Movement Biomechanics Laboratory (200 Lees Avenue, E020). You will be asked to perform a series of overground walking tasks in the laboratory, a quiet standing task, a six-minute walk on a treadmill at your preferred walking pace, a six-minute walk test in the hallway near the laboratory, walk a loop consisting of a stair ascent, a flat walk, and a stair descent (~146 metres), and perform a six-minute walk test outside.

Upon arrival, your height and weight will be measured and you will be asked to change into a custom-made Lycra shirt and your personal athletic shorts. Afterwards, you will be outfitted with a 17-sensor IMU suit, which will be adhered to your body using neoprene bands and a custom shirt; IMUs will be placed on your lower limbs, upper limbs, trunk, pelvis, and head. These sensors will then connect to an on-board computer that will stream all the IMU data to the data collection computer. You will also be outfitted with two smart shoe insoles, which will be inserted into your shoes. Before the experimental trials can begin, you will be asked to perform a calibration procedure, for both the IMU system and the smart insoles. For the insoles, you will be asked to stand on one foot for five seconds and then stand on the other foot for five seconds. For the IMU system, you will be asked to stand in a neutral posture (N-pose), walk for five seconds forward, turn around, and return to an N-pose at the origin. After these calibration trials are completed, the experimental trials will begin.

Possible Risks and Discomforts:

There are no significant risks associated with participating in this study. You may experience fatigue due to the nature of the tasks; however, sufficient rest will be given to reduce these effects. Tape may be used to adhere some loose wires that may cause minor skin irritation; similar to what it experienced with a bandage and typically fades within 2 to 3 days.

Should you experience any major discomfort, please tell us immediately and seek primary care from a medical professional on campus (100 Marie Curie, Ottawa, Tel.: 613-564-3950) or a medical professional of your choosing.

Possible Benefits:

You will not directly benefit from participating in this study. However, the results of this study will greatly add to the quality of life of individuals living with MS.

Voluntary Participation:

You are not obliged to participate in this study; your participation is voluntary. You may withdraw from the study at any time with no penalty or coercion. You may ask to stop the movement protocol at any time due to fatigue or discomfort; adequate rest will be provided and the collection can be terminated if necessary. You may withdraw from the study at any time with no penalty or coercion. There are no social obligations to participating nor will there be any social or academic penalties that will prevent you from withdrawing from the study at any point.

Confidentiality:

All personal information is kept confidential. Information gained from this study will be stored electronically and will need a password to access, which will only be known to Dr. Ryan Graham, Matthew Mavor and Alexandre Mir-Orefice. Paper study records are stored in a locked cabinet and will be destroyed after 5 years post publication; electronic records will be deleted and paper records will be shredded. You will not be identified by name in any reports of the completed

study. Your anonymity will be strictly maintained – you will not be identified by your name, but will be determined by an independent study number.

Compensation:

You will receive a \$25 gift card to a business of your choice as compensation for your participation in this study. If you chose to withdraw from the study for any reason, you will be fully compensated.

Questions about the Study:

You are free to ask questions at any time during and after the protocol and by contacting the principal investigator by email: Dr. Ryan Graham (ryan.graham@uottawa.ca). The ethical components of this research project has been approved by the University of Ottawa research ethics board. If you have any questions regarding the ethical conduct of this study, you may contact the Protocol Officer for Ethics in Research, University of Ottawa, Tabaret Hall, 550 Cumberland Street, Room 154, Ottawa ON, K1N 6N5. Tel.: (613) 562-5387 Email: ethics@uottawa.ca. There are two copies of the consent form, one of which is yours to keep.

Research Project Title: Development of a gait detection algorithm for individuals with multiple sclerosis

Consent:

I have read this consent form, and I agree to participate in the procedures of this study.

Printed Name of Participant

Signature of Participant

Date

Investigator Statement (or Person Explaining the Consent):

I have carefully explained to the research participant the nature of the above research study. To the best of my knowledge, the research participant signing this consent form understands the nature, demands, risks and benefits involved in participating in this study. I acknowledge my responsibility for the care and well-being of the above research participant, to respect the rights and wishes of the research participant, and to conduct the study according to applicable Good Clinical Practice guidelines and regulations.

Name of Investigator/Delegate (printed)

Signature of Investigator/Delegate

Date

Informed Consent to have Pictures and Videos Taken:

I consent to have side view pictures taken of myself completing the experiment, and understand that no pictures will be taken at any point without me knowing. I also understand that if any of these pictures are used in a subsequent presentation or publication, that my face and any other identifiers will be blurred. Video recordings will be used to track your movement patterns using (Theia 3D). Any videos used for presentations will be anonymized by only using the resulting skeleton/skeleton video overlay. You cannot participate in the research study without consenting to have pictures and videos taken.

Name

Date

Signature

Witness Name

Witness Signature

Future Participation:

- I am interested in being contacted to participate in future research performed by this laboratory (your email information will be saved in a password protected file).

Appendix B: Anthropometric measurements

Table D.1 Anthropometric measurements for the Xsens MVN Link motion capture suit.

Measure	Description
Body height	From ground to top of the head
Foot size	From the back of the heel to the front of the toes
Arm span	From fingertip to fingertip with straight arms in 90° shoulder abduction
Ankle height	From the floor to the center of the ankle
Hip height	From the floor to the greater trochanter
Hip width	Distance between the left and right anterior superior iliac spine
Knee height	From the floor to the lateral epicondyle
Shoulder width	Distance between the left and right acromion
Shoulder height	From the floor to the C7 spinal process
Elbow span	From the right to the left olecranon in T-pose
Wrist span	From the right to the left ulnar styloid in T-pose

Appendix C: Instrumented insole design

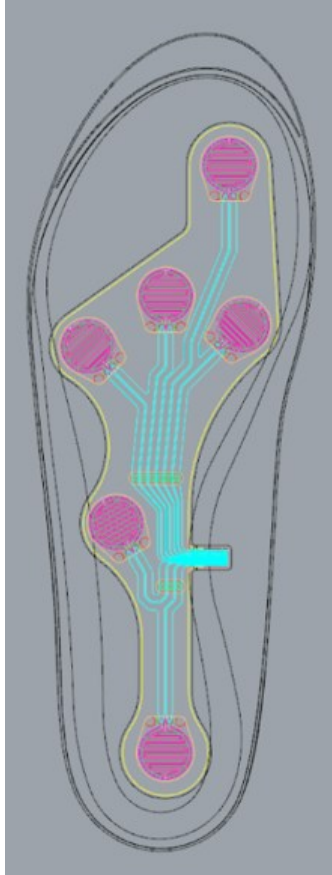


Figure C.1 Instrumented insole plantar pressure sensor placement.

Appendix D: Median Absolute Deviation of Yaw Variability Calculation

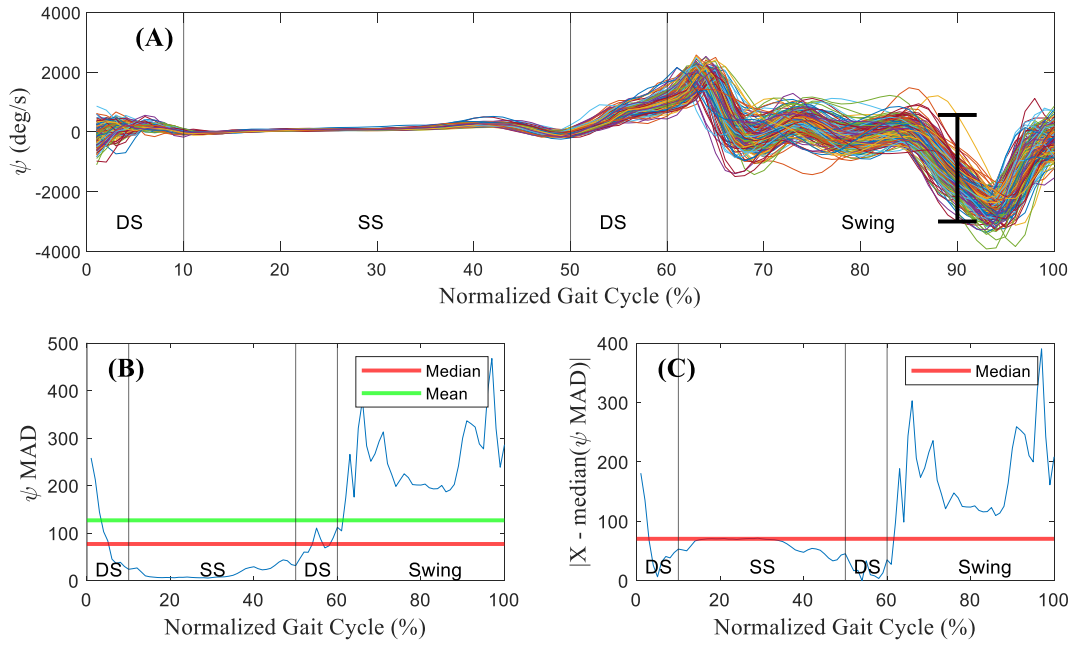


Figure D.1 Mean and median absolute deviation of yaw (ψ) variability calculation. (A) Overlay of raw ψ values over the normalized gait cycle with black bar to illustrate dispersion; (B) ψ MAD across the normalized gait cycle with mean and median values; (C) absolute value of the difference between ψ MAD and the median of ψ MAD with median.

Abbreviations: DS: Double support; SS: Single support; MAD: Median absolute deviation.

Appendix E: List of Metrics

Table E.1 List of spatiotemporal variability, raw kinematic variability, and stability metrics.

Spatiotemporal variability metrics	Raw kinematic variability metrics	Stability metrics
Stride time mean	Anteroposterior acc mean	Insole foot LDS
Stride time SD	Anteroposterior acc SD	IMU foot LDS*
Stride time CoV	Anteroposterior acc CoV	IMU trunk LDS* ⁺
Stride time MAD	Anteroposterior acc MAD	
Stance time mean	Mediolateral acc mean	
Stance time SD	Mediolateral acc SD	
Stance time CoV	Mediolateral acc CoV	
Stance time MAD	Mediolateral acc MAD	
Swing time mean	Vertical acc mean	
Swing time SD	Vertical acc SD	
Swing time CoV	Vertical acc CoV	
Swing time MAD	Vertical acc MAD	
SS time mean	Magnitude of acc mean	
SS time SD	Magnitude of acc SD	
SS time CoV	Magnitude of acc CoV	
SS time MAD	Magnitude of acc MAD	
DS time mean	Pitch angvel mean	
DS time SD	Pitch angvel SD	
DS time CoV	Pitch angvel CoV	
DS time MAD	Pitch angvel MAD	
Step time mean ⁺	Roll angvel mean	
Step time SD ⁺	Roll angvel SD	
Step time CoV ⁺	Roll angvel CoV	
Step time MAD ⁺	Roll angvel MAD	
Cadence mean ⁺	Yaw angvel mean	
Cadence SD ⁺	Yaw angvel SD	
Cadence CoV ⁺	Yaw angvel CoV	
Cadence MAD ⁺	Yaw angvel MAD	
Stride length mean	Magnitude of angvel mean	
Stride length SD	Magnitude of angvel SD	
Stride length CoV	Magnitude of angvel CoV	
Stride length MAD	Magnitude of angvel MAD	
Stride velocity mean		
Stride velocity SD		
Stride velocity CoV		
Stride velocity MAD		

Abbreviations: SD = Standard deviation; CoV = Coefficient of variation; MAD = Median absolute deviation; SS = Single support; DS = Double support; acc = acceleration; angvel = angular velocity; LDS = local dynamic stability; IMU = inertial measurement unit

Note: IMU foot LDS and IMU trunk LDS were not included as potential predictor variables in the multiple linear regression model.

Note: *: Non-predictor variable, ⁺: Identical value for left and right side.